

Siphonophore Phylogeny

Stefan Siebert^{1,2}, Felipe Zapata^{1,3}, Mark Howison⁴, Cat Munro¹, Alejandro Damian Serrano¹, Samuel H Church^{1, 5}, Freya Goetz^{1,5}, Phil Pugh, Steven H.D. Haddock⁴, Casey W. Dunn^{1*}

¹ Department of Ecology and Evolutionary Biology, Brown University, Providence, RI, USA

² Current address: Department of Molecular & Cellular Biology, University of California at Davis, Davis, CA, USA

³ Current address: Department of Ecology and Evolutionary Biology, University of California Los Angeles, Los Angeles, CA, USA

⁴ Brown Data Science Practice, Brown University, Brown University, Providence, RI, USA

⁵ Harvard

⁵ Current address: Smithsonian, Washington DC, USA

⁴ Monterey Bay Aquarium Research Institute, Moss Landing, CA, USA

* Corresponding author, casey_dunn@brown.edu

Abstract

Introduction

Siphonophores are...

Methods

This manuscript is an executable document computed directly from the data, providing an explicit and reproducible description of all findings. All scripts for the analyses are available in a git repository at https://github.com/caseywdunn/siphonophore_phylogeny_2017. The most recent commit at the time of the analysis presented here was 6bd0e9f1fcf5e8a1b56b7b00531609965d3d8e34.

Collecting

Collection data on all examined specimens, a description of the tissue that was sampled from the colony, collection mode, sample processing details, mRNA extraction methods, sequencing library preparation methods and sequencing details are summarized in supplementary table 1. Monterey Bay and Gulf of California specimens were collected by remotely operated underwater vehicle (ROV) or during blue-water scuba dives. *Chelophyes appendiculata* and *Hippopodius hippopus* specimens were collected in the bay of Villefranche-sur-Mer, France, during a plankton trawl on 04/13/11. Available physical vouchers have been deposited at the Museum of Comparative Zoology (Harvard University), Cambridge, MA, and at the United States National Museum (Smithsonian Institution), Washington, DC. Accession numbers are given in supplementary table X. In cases where physical vouchers were unavailable we provide photographs to document species identity (table x).

Sequencing

When possible specimens were starved overnight in filtered seawater at temperatures close to ambient water temperatures at the time point of specimen collection (supplementary table 1). mRNA was extracted directly from tissue using a variety of methods (supplementary table x): Magnetic mRNA Isolation Kit (NEB, #S1550S), Invitrogen Dynabeads mRNA Direct Kit (Ambion, #61011), Qymo Quick RNA MicroPrep (Zymo

#R1050), or from total RNA after Trizol (Ambion, #15596026) extraction and through purification using Dynabeads mRNA Purification Kit (Ambion, #61006)- in case of very small total RNA quantities, only a single round of bead purification was performed; or Trizol directly into the Illumina TruSeq Stranded Library Kit. Extractions were performed according to the manufacturer’s instruction. Any resulting higher rRNA read counts were dealt with further downstream in the bioinformatics workflow. Libraries were prepared for sequencing using the Illumina TruSeq RNA Sample Prep Kit (Illumina, #FC-122-1001, #FC-122-1002), the Illumina TruSeq Stranded Library Prep Kit (Illumina, #RS-122-2101) or the NEBNext RNA Sample Prep Master Mix Set (NEB, #E6110S). We collected long read paired end Illumina data for *de novo* transcriptome assembly. In the case of large tissue inputs, libraries were sequenced separately for each tissue and subsequently were subsampled and pooled *in silico*. Libraries were sequenced on the HiSeq 2000, 2500, and 3000 sequencing platforms (supplementary table 1). Summary statistics for expression libraries are given in Table 1.

Analysis

New data were analysed in conjunction with 13 publically available datasets, with a total number of 43 species. Sequence assembly, annotation, Maximum Likelihood (ML) phylogenetic analysis were conducted with the tool Agalma (Dunn et al. 2013), v. 1.00, and Bayesian Inference (BI) analyses were conducted using Phylobayes (Lartillot et al. 2009) v. 1.7a-mpi. Source code for all analysis steps, sequence alignments, sampled and consensus trees, and voucher information are available in a git repository https://github.com/caseywdunn/siphonophore_phylogeny_2017.

In the final analyses, we sampled 1,071 genes to generate a supermatrix with 60% occupancy and a length of 378,468 amino acids. Two outgroup species, *Atolla vanhoeffeni* and *Aegina citrea*, were removed from the final supermatrix and phylogeny due to low gene occupancy (gene sampling of 20.8% and 14.5% respectively in a 50% occupancy matrix with 2,203 genes). ML analyses were conducted on the unpartitioned supermatrix using the WAG+ γ model of amino acid substitution, and bootstrap values were estimated using 1000 replicates. BI was conducted using two different CAT models, CAT-Poisson and CAT-GTR (Lartillot and Philippe 2004). Two independent MCMC chains were run under the CAT-GTR model, and four independent MCMC chains were run under the CAT-Poisson model. The CAT-GTR and CAT-poisson models did not converge after a long CPU time, and only the results from the CAT-poisson model are included here.

Subsequent analyses were conducted in R and integrated into this manuscript with the **knitr** package. See Supplementary Information for R package version numbers.

Hypothesis testing

Results and Discussion

Sample collecting and sequencing

Table 1 (at the end of file): Summary statistics for libraries.

Species phylogeny

(XX This paragraph on sampling through Agalma analyses) The analyses presented here consider XXX siphonophore species and 8 outgroup species. This includes new data for XXX species. Summary stats on assemblies XX (Table XX). Matrix has XX genes, XX sites, and occupancy is XX.

(XX This paragraph on summarizes phylogeny runs, apart from tree topology) Maximum likelihood analyses had 1000 replicates. We ran 4 phylobayes chains, and visual inspection of the traces indicated that a burn in of 400 trees was sufficient for all runs. This left 15847 trees in the posterior. XXConvergence...

These findings are entirely consistent with a previous analysis based on two genes (16S and 18S ribosomal RNA) (Dunn et al. 2005). Cystonectae is the sister group to the remaining siphonophores, and Calyophorae

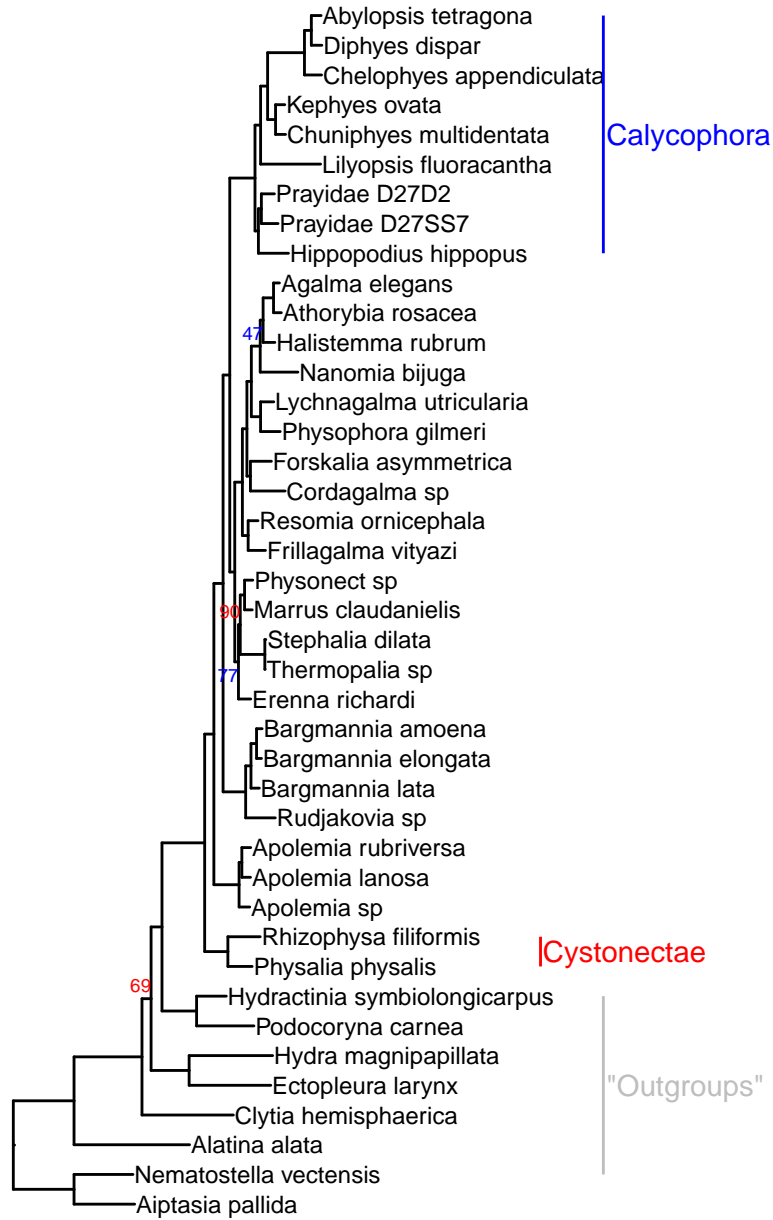


Figure 1: Phylogram of siphonophore relationships. Node labels indicate bootstrap support percent, unnumbered nodes have 100% support. The image was rendered with ggtree (Yu et al. 2016)

is nested within the paraphyletic “Physonectae”. In addition, multiple nodes that were not resolved in the previous two-gene analysis do receive strong support in this 1,071-gene transcriptome analysis. These findings include XXX.

Character Evolution

Siphonophores have evolved a fascinating diversity of morphological features, zooid types, life history traits, and habitats. Here we explore the evolutionary history of some of these features.

In our previous siphonophore phylogenetic analysis (Dunn et al. 2005) there were several characters left with equivocal evolutionary histories, due to unresolved relationships between physonects. With our current cladistic resolution, we were able to determine the following results:

Evolution of Monoecy

[Citation needed] noticed for the first time that some siphonophores were monoecious and others were dioecious. Our analyses in 2005 reconstructed this character and found a great amount of phylogenetic conservatism, with an unambiguous resolution of the MRCA as dioecious, and the appearance of monoecy in several taxa and clades (including Calyptophorae) within the polytomy. Figure X shows the evolution of sex distribution in siphonophores under the current better-resolved tree model, and it strongly indicates that monoecy in siphonophores from a dioecious ancestor occurred twice, in the branch leading to Calyptophorae and in the branch leading to Agalmatids (sensu lato). There is a small probability for an alternative scenario featuring a single gain of monoecy before the split of Calyptophorae, with a subsequent derived shift back to dioecy in the *Marrus-Erenna* clade.

The Evolution of Zooid Types

One of the most striking aspects of siphonophore biology is their diversity of unique zooid types. Other colonial cnidarians (such as Hydractinia) and some bryozoans (example) have been found to have up to X different zooid types [Citation1, Citation 2]. The siphonophore genus *Forskalia* has 6 basic zooid types (pneumatophore, nectophore, gastrozooid, palpon, bract, and gonophore), and a total of 10 counting subtypes (4 types of bract, male & female gonophores). Diphyomorphs have more than 1 type of nectophore, while Cystonects have none. Here we reconstruct the evolutionary origins of the different zooid types and subtypes on the present transcriptome tree.

Nectophores are retained modified medusae Codonophora use for swimming. The nectosome is the region of the colony that develops from the nectosomal growth zone. Unlike the siphosomal growth zone, the nectosome does not bud gastrozooids, but nectophores (and in the case of *Apolemia*, also palpons). In fact, with the exception of *Physalia physalis* (which grows small nectophores near the gonodendra), siphonophore nectophores are exclusively found on the nectosome. It is likely that the MRCA of siphonophores had a nectosome, which was lost on the branch leading to Cystonects. We cannot exclude with certainty the alternative hypothesis of a nectosome-less ancestor followed by a gain of the nectosome in the branch leading to the Codonophora. The nectosome probably arose as a duplication of the siphosome, followed by functional specialization in propelling the colony. Figure X shows the origin of the dorsal nectosome in the Agalmatidae (sensu stricto) from an ancestral ventral nectosome.

All Codonophora have a nectosome, but the number and subtypes of nectophores present varies greatly between species. As shown in Figure X, most Codonophora presents the ancestral nectosome with multiple nectophores of the same subtype. However, Calyptophorans evolved a different system with just 2 nectophores of one type. This shift may be associated with the loss of the pneumatophore. Not all Calyptophorans remained with this arrangement. The Hippopodidae returned to bearing multiple identical nectophores, many of which are inactive and serve functions of defense (like a shell to retract in) and buoyancy. As in the rest of Calyptophorans, the Hippopodids only use 2 nectophores to propel the colony. Another interesting shift

occurs in the branch leading to Diphyomorpha, where the 2 nectophores specialize into 2 subtypes, associated with a shift into a vertically aligned position and pointed bell shapes. The 2 types function together in a coupled hydrodynamic system that allows very fast escape responses (Mackie 1964).

Bracts also present a complex evolutionary history of subtypes (Figure X). Bracts are highly reduced zooids unique to siphonophores, but they are only present in the Codonophora. As with the nectosome, we have ambiguity determining whether the MRCA of siphonophores had bracts or not. The MRCA of Codonophora had only one bract subtype, which was lost in Hippopodidae and independently evolved into 2 subtypes in *Erenna* and *Nanomia*. During the branch leading to Forskalidae, bract subtypes evolved from 1 to 4 morphologically distinct forms. Bracts are important for protection of the delicate zooids and to help maintain neutral buoyancy. Some calyphorans are able to actively regulate the Na/NH₄ balance to adjust their buoyancy (ref).

The ancestral siphonophore certainly had a pneumatophore (Figure X). This zooid type helps the colony float, maintain its pose, and regulate geotaxis (Church, 2013). Despite its diverse biological functions, it is lost in Calyphorae and never gained again in that clade. Calyphorans rely on the ionic balance of their gelatinous nectophores and bracts to retain posture and neutral buoyancy.

Palpons are modified mouthless gastrozooids used for digestion and circulation of the gastrovascular fluid. They were present in the MRCA of siphonophores (Figure X), retained in most species, but lost twice independently in the branches leading to *Bargmannia* and Calyphorae. These taxa must have found other avenues to effectively circulate nutrients across the colony.

The Gain and Loss of Tentilla

The most complex nematocyst batteries of Cnidaria can arguably be found among the siphonophores, hanging in regularly spaced tentacle side branches called tentilla. Most hydrozoans, including the clade that contains siphonophores, bear simple tentacles (tentacles with no side branches). It is still an open question whether the most recent common ancestor (MRCA) of Siphonophora had simple or branched tentacles. The only two siphonophore genera regarded as lacking tentilla are *Physalia* and *Apolemia*, at each side of the earliest split in the siphonophore tree, with an immediate sister group with all members bearing tentilla (*Rhizophysidae* and *{Bargmannia, Diphyes}*) (FigXX). Figure X shows the evolution of this character on the current phylogeny, indicating a most-likely tentilla bearing MRCA, with two independent losses. However, this reconstruction bears some uncertainty on the state of the MRCA, suggesting a ~30% probability of 2 independent gains of tentilla in the branches leading to *Rhizophysidae* and *{Bargmannia, Diphyes}*.

A key issue here is how we code for absence of tentilla, especially for the case of *Physalia physalis*. The tentacles of this species, when uncoiled, show very prominent, evenly spaced, 3D buttons which contain all active and functionally arranged nematocysts used by the organism for prey capture. Siphonophore tentilla are complete diverticular branchings of the tentacle ectoderm, mesoglea, and gastrovascular canal (lined by endoderm). Hessinger & Ford 1988 (in the Biology of Nematocysts) described these bands as enclosing individual fluid-filled chambers connected by narrow channels to the tentacular canal, lined by endoderm. This suggests they are not just ectodermal swellings, but probably are reduced tentilla. When we code *Physalia physalis* as tentilla bearing, the results for the character reconstruction change to a more parsimonious scenario (Figure X), indicating there was a single loss of tentilla in the branch leading to *Apolemiidae*. This result suggests an unambiguous tentilla-bearing state of the MRCA.

The Evolution of Vertical Habitat Use

Siphonophores are abundant predators in the pelagic realm, ranging from the surface (*Physalia physalis*) to bathypelagic depths (ref, *Bargmannia* sp 3888m VARS unpublished). While there are some pleustonic (*Physalia*) and benthic (*Rhodaliidae*) siphonophores, the phylogeny suggests the siphonophore MRCA was planktonic, as most extant taxa are. Some interesting questions arise from these facts, including 1) what was the bathymetric niche of the siphonophore MRCA, and 2) how did siphonophore's vertical habitat use of the water columns evolve along the phylogeny. Our results indicate a mesopelagic MRCA, with several

convergent transition events to epipelagic and bathypelagic waters. There was only a single transition to benthic lifestyle on the stem of *Rhodaliidae*.

Discussion

The strong phylogenetic signal in the characters traditionally used for taxonomic diagnostics is a positive indicator of the applicability and unambiguity of these characters.

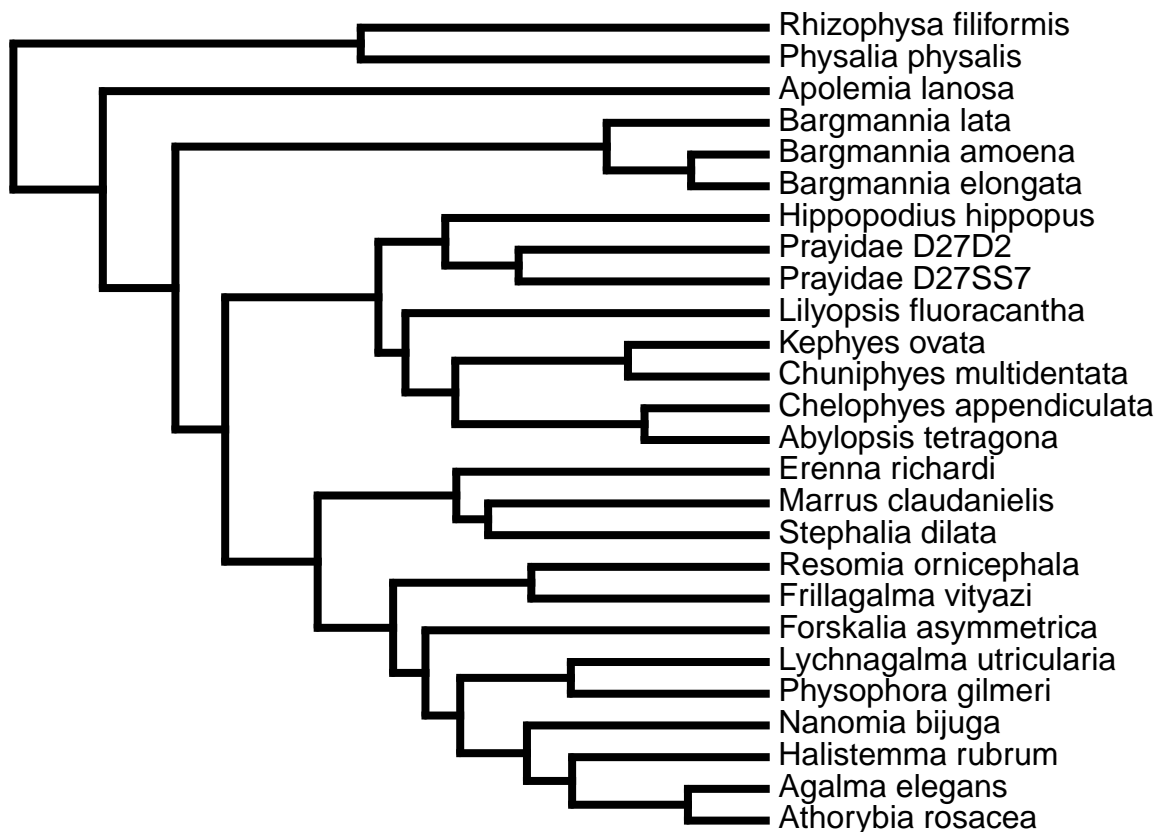
Conclusions

Acknowledgements

This work was supported by the National Science Foundation (DEB-1256695 and the Waterman Award). Sequencing at the Brown Genomics Core facility was supported in part by NIH P30RR031153 and NSF EPSCoR EPS-1004057. Data transfer was supported by NSF RII-C2 EPS-1005789. Analyses were conducted with computational resources and services at the Center for Computation and Visualization at Brown University, supported in part by the NSF EPSCoR EPS-1004057 and the State of Rhode Island. We also thank the MBARI crews and ROV pilots for collection of the specimens.

Supplementary Information

Supplementary Analyses

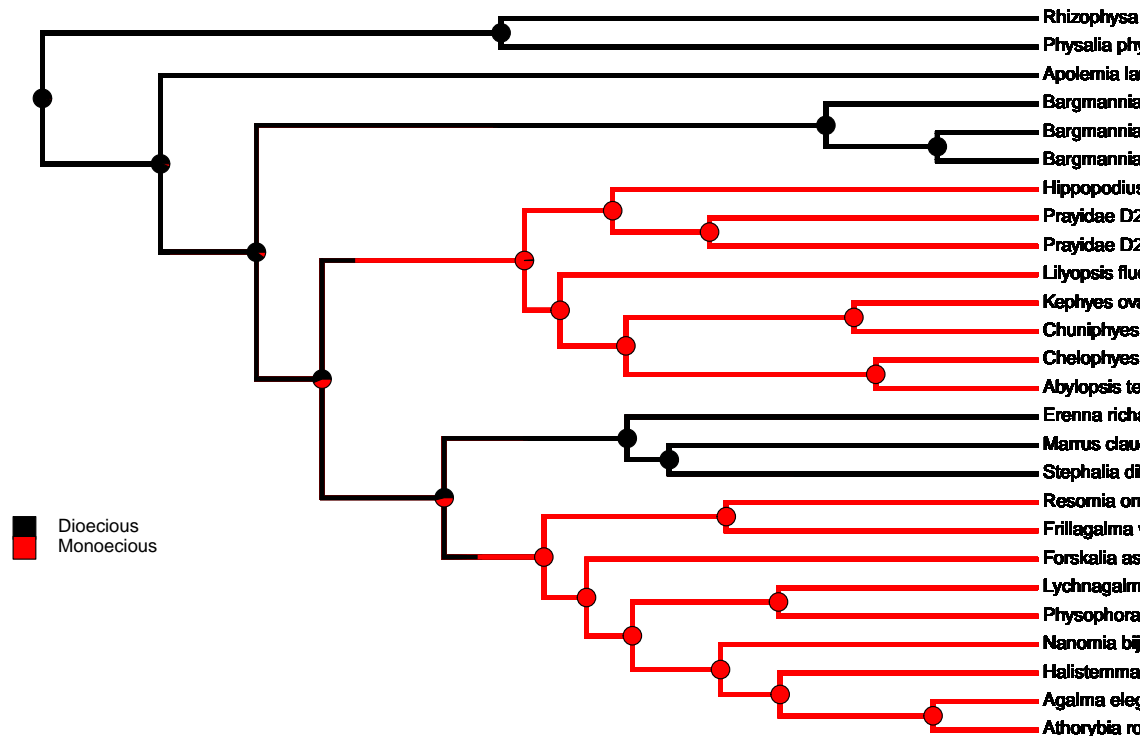


The Tree:

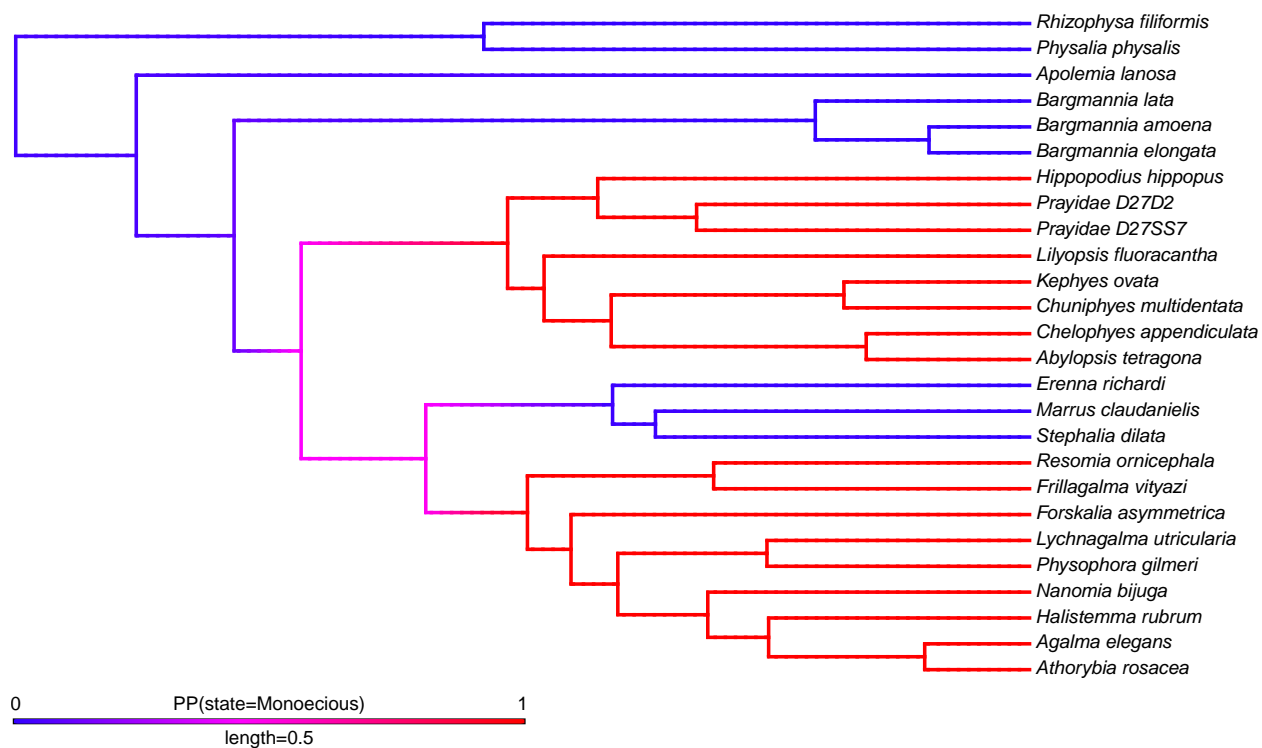
Stochastic trait mapping:

```
## [1] "SIMMAP Sex Distribution"
## [1] "SIMMAP Palpons"
## [1] "SIMMAP Tentilla"
## [1] "SIMMAP Tentilla2"
## [1] "SIMMAP Nectosome"
## [1] "SIMMAP Nectosome Position"
## [1] "SIMMAP Nectophore Types"
## [1] "SIMMAP Pneumatophore"
## [1] "SIMMAP Bract Types"
## [1] "SIMMAP Habitat"
```

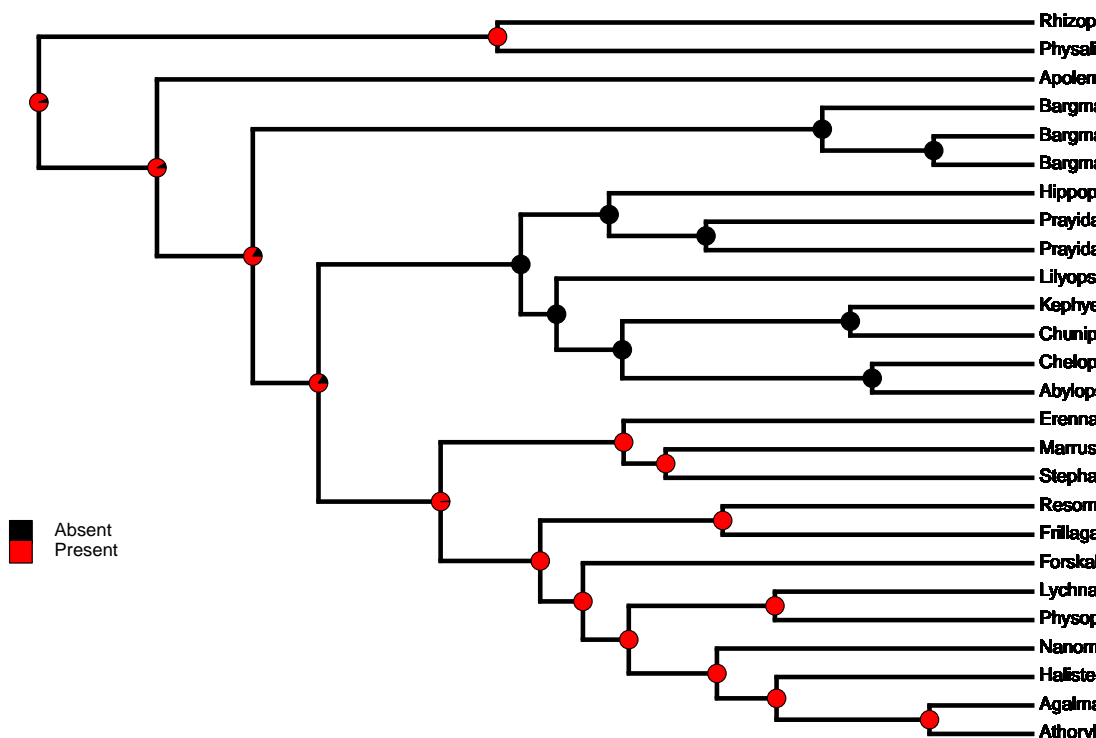
When we reconstruct the evolutionary history of different traits in siphonophore species, we obtain the following results:



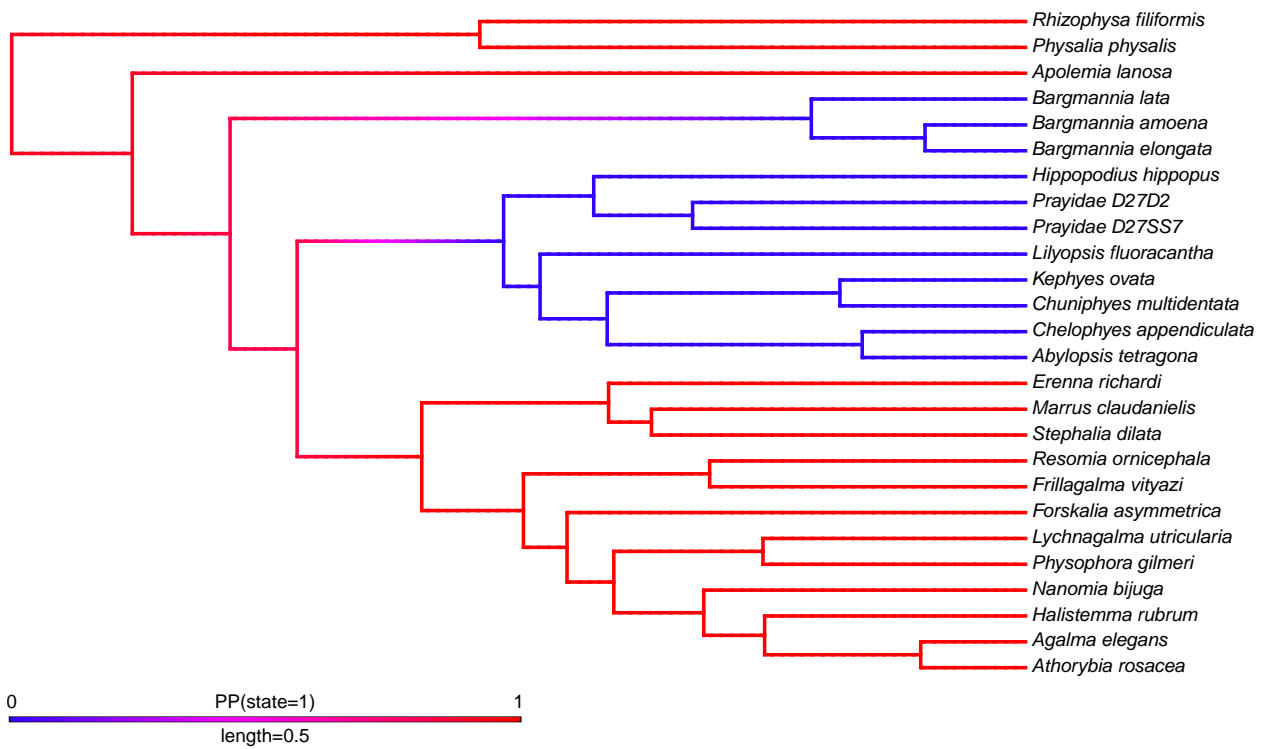
SIMMAP Sex distribution:



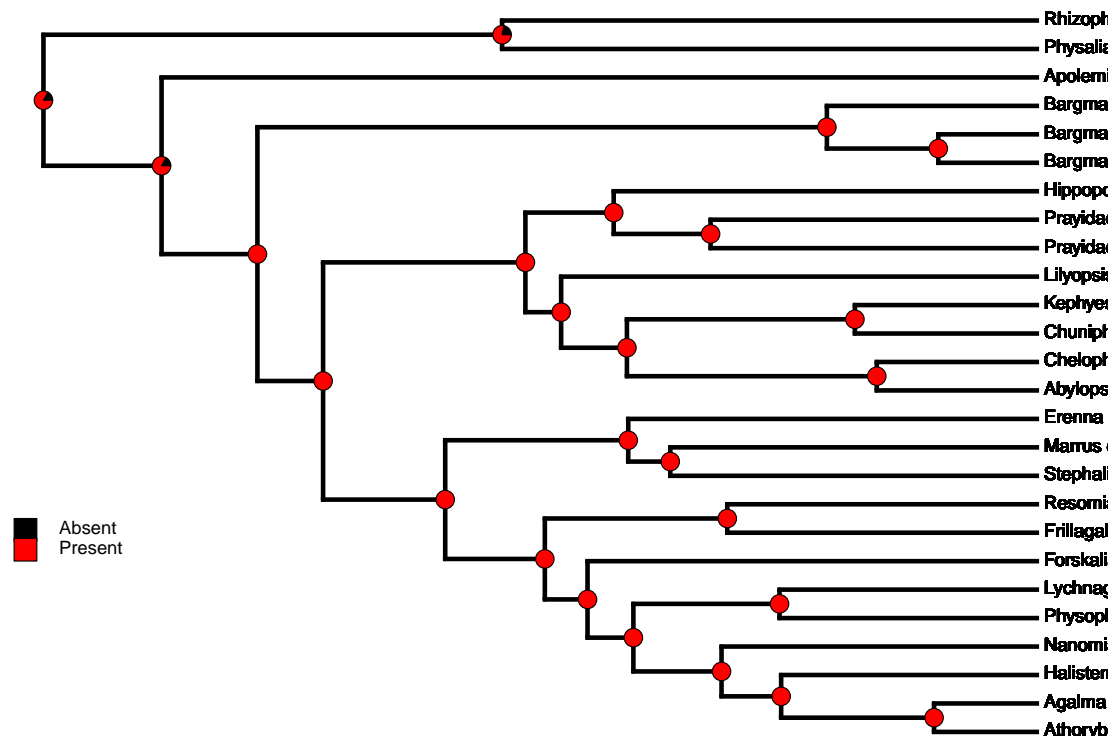
Posterior probabilities of states (0 Dioecious, 1 Monoecious).



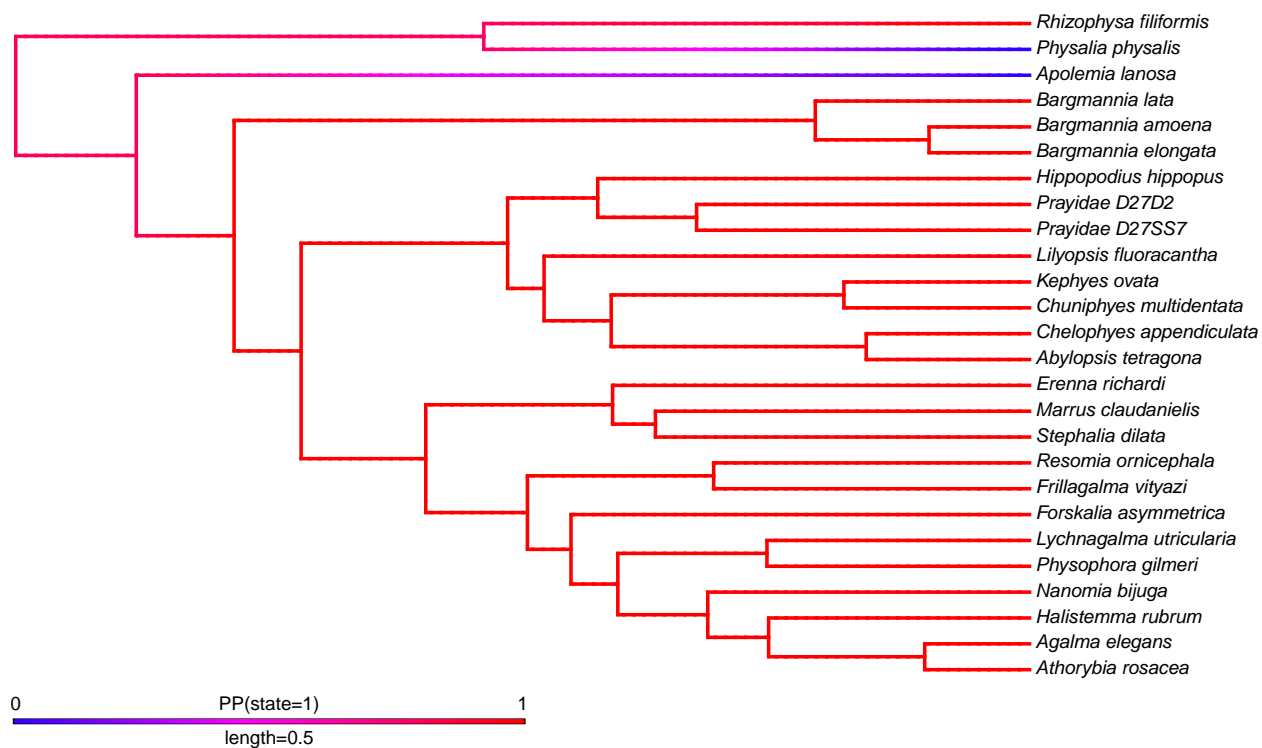
SIMMAP Presence of palpons:



Posterior probabilities of states (1 Present, 0 Absent).

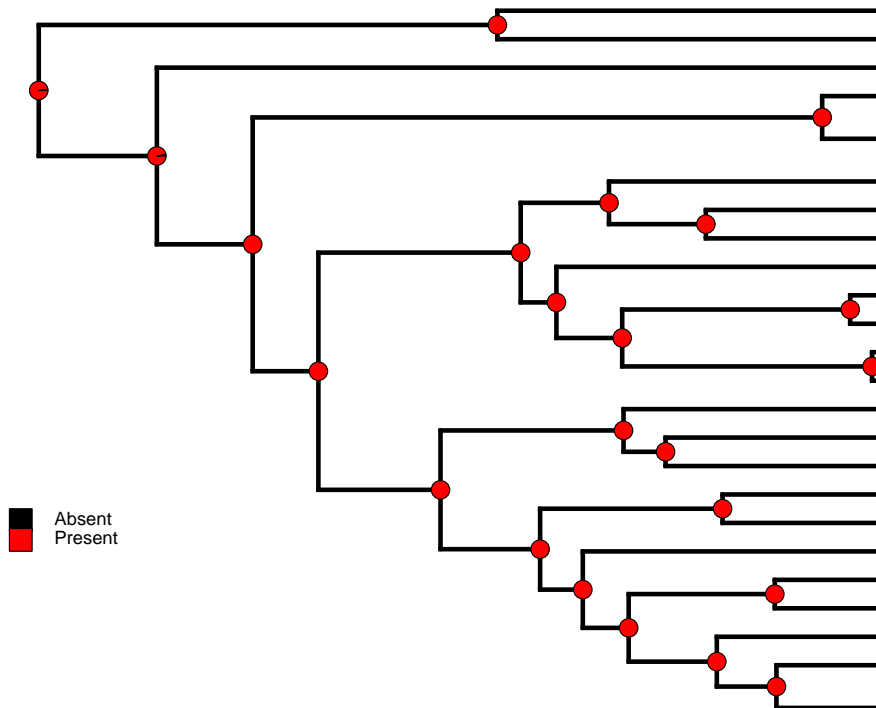


SIMMAP Presence of tentilla:

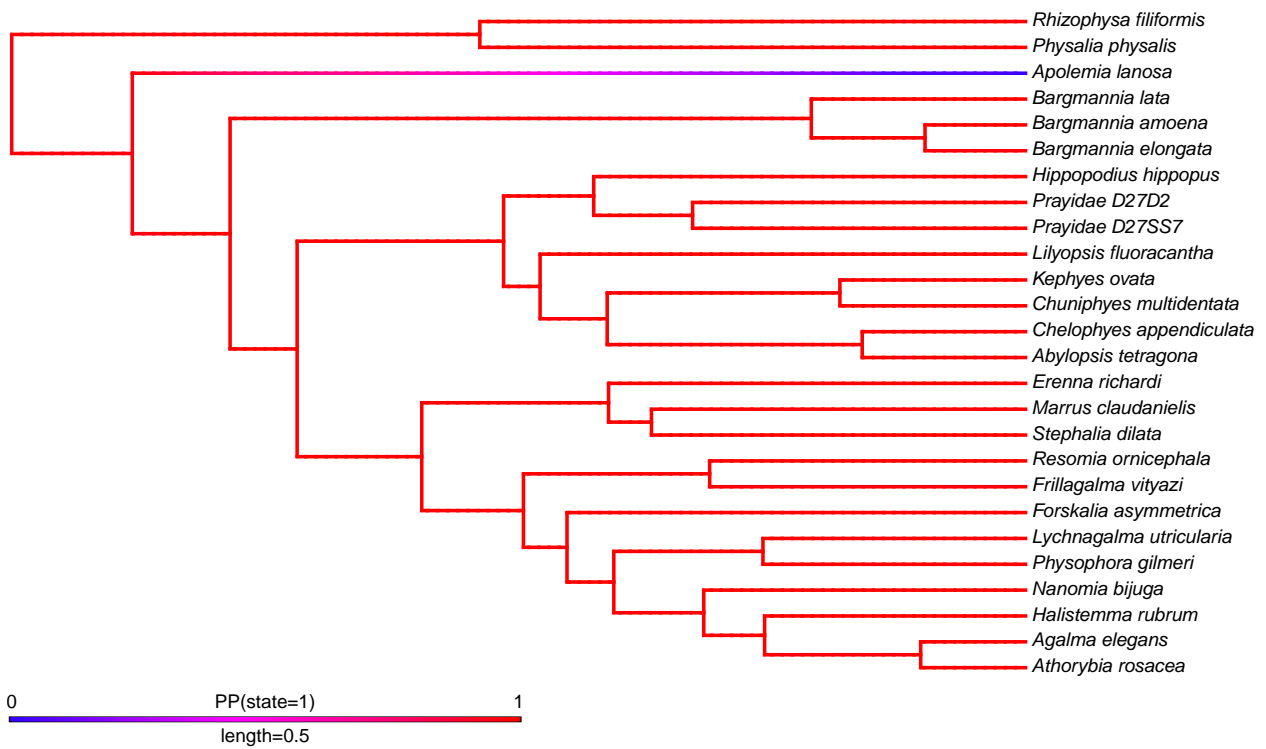


Posterior probabilities of states (1 Present, 0 Absent).

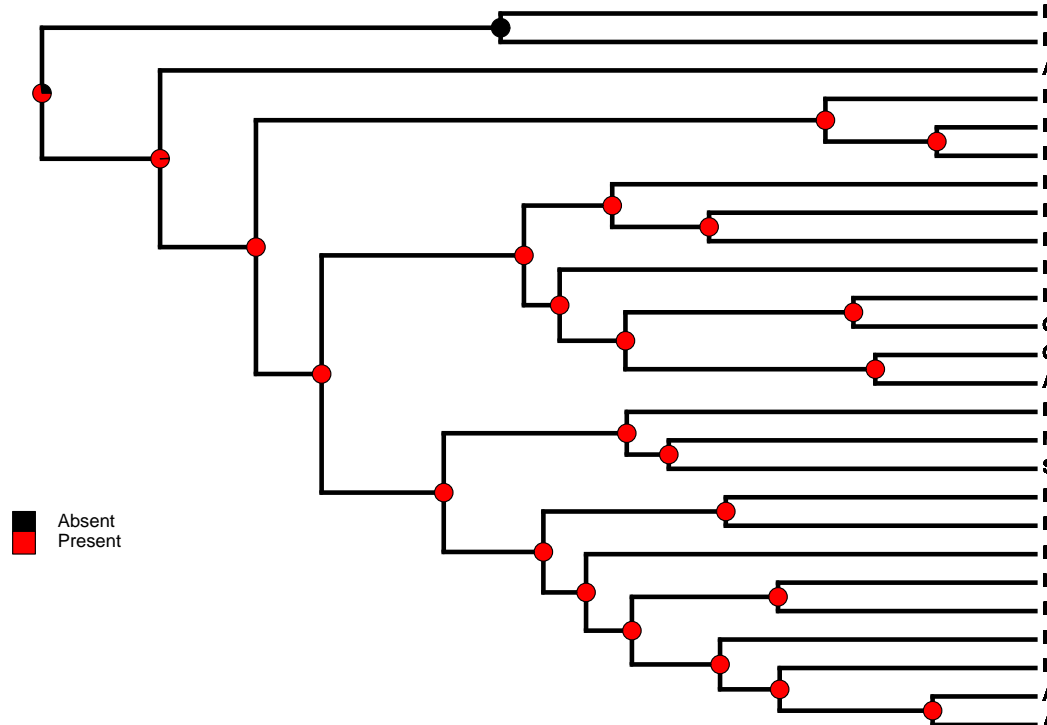
Physalia physalis may have reduced tentilla, which would indicate there was only one loss of tentilla at the branch leading to *Apolemia*.



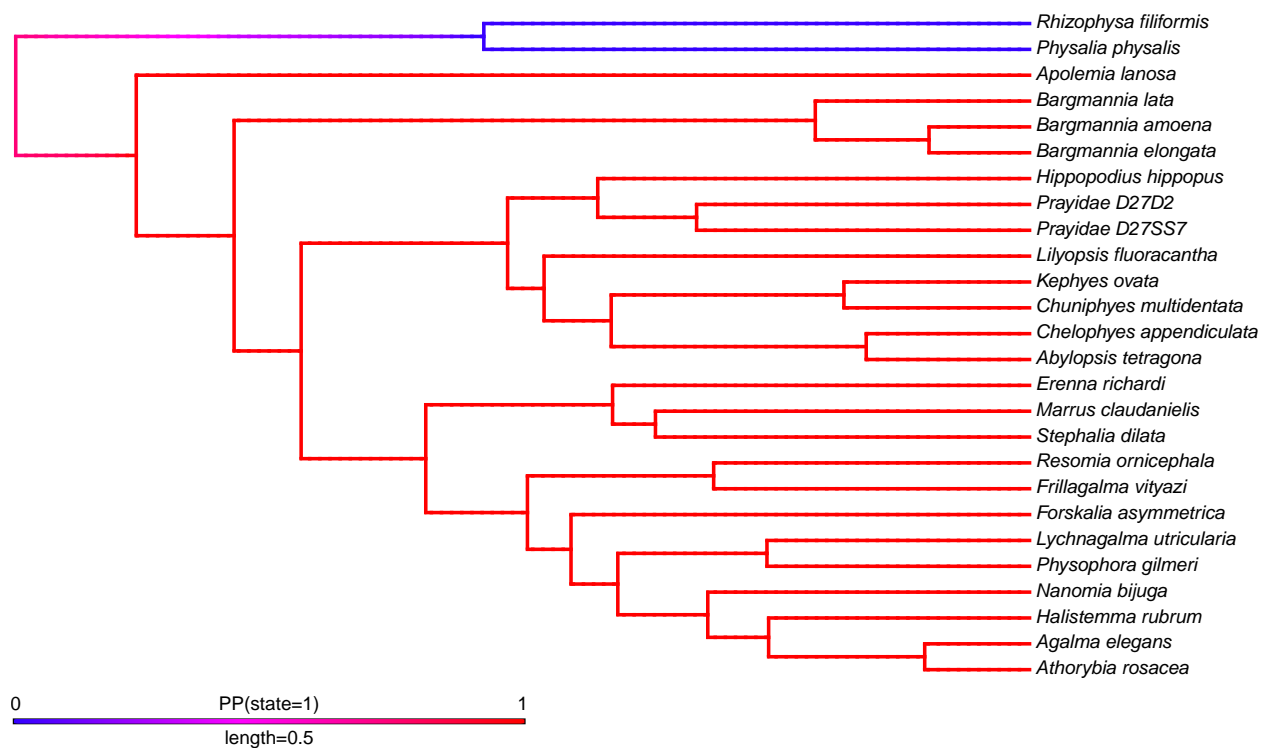
SIMMAP Presence of tentilla - *Physalia* corrected:



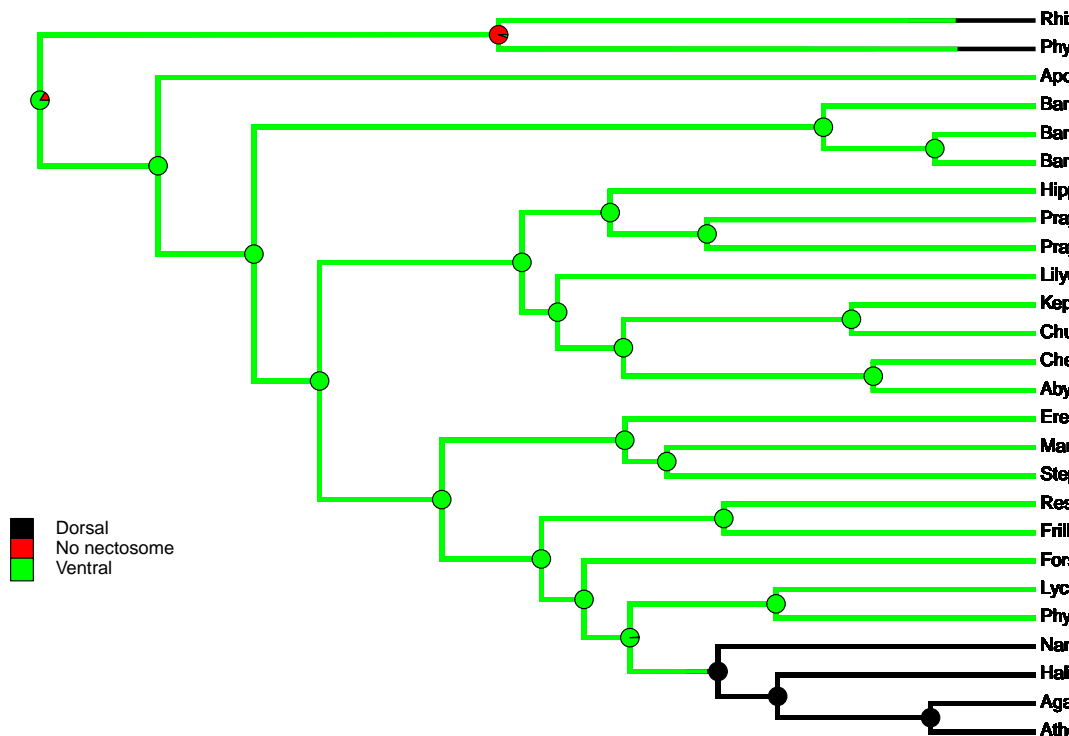
Posterior probabilities of states (1 Present, 0 Absent).



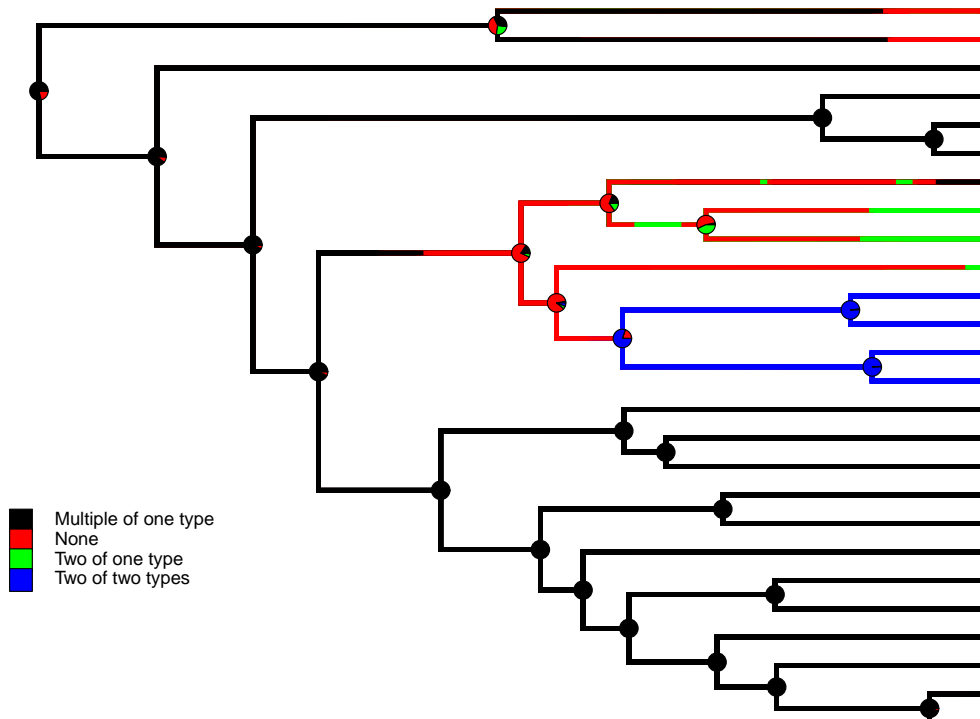
SIMMAP Presence of Nectophores:



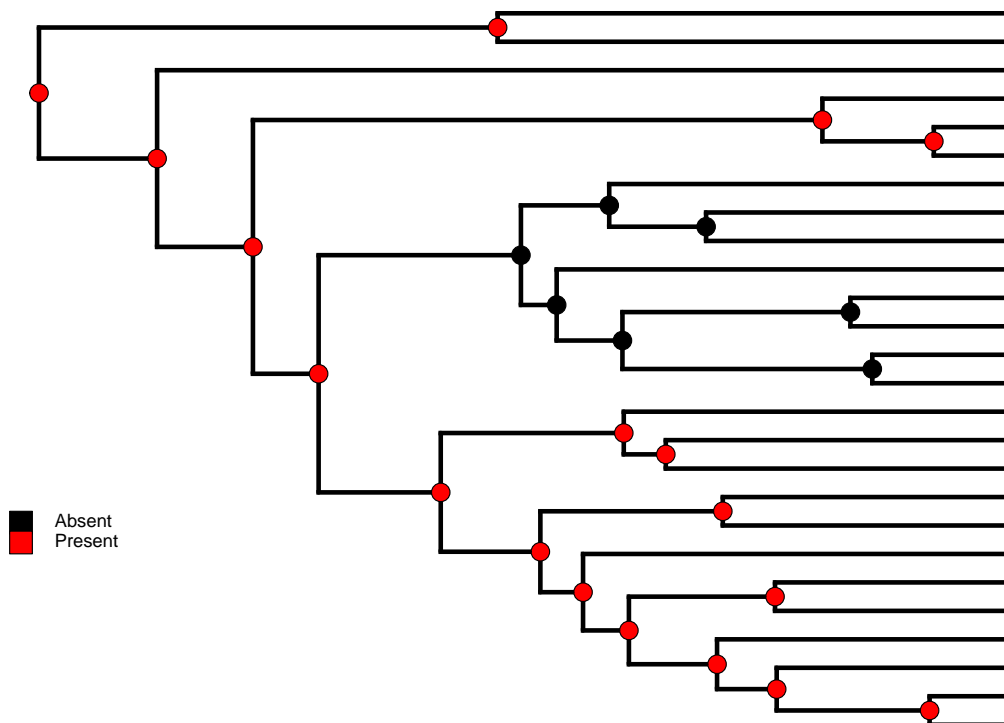
Posterior probabilities of states (1 Present, 0 Absent).



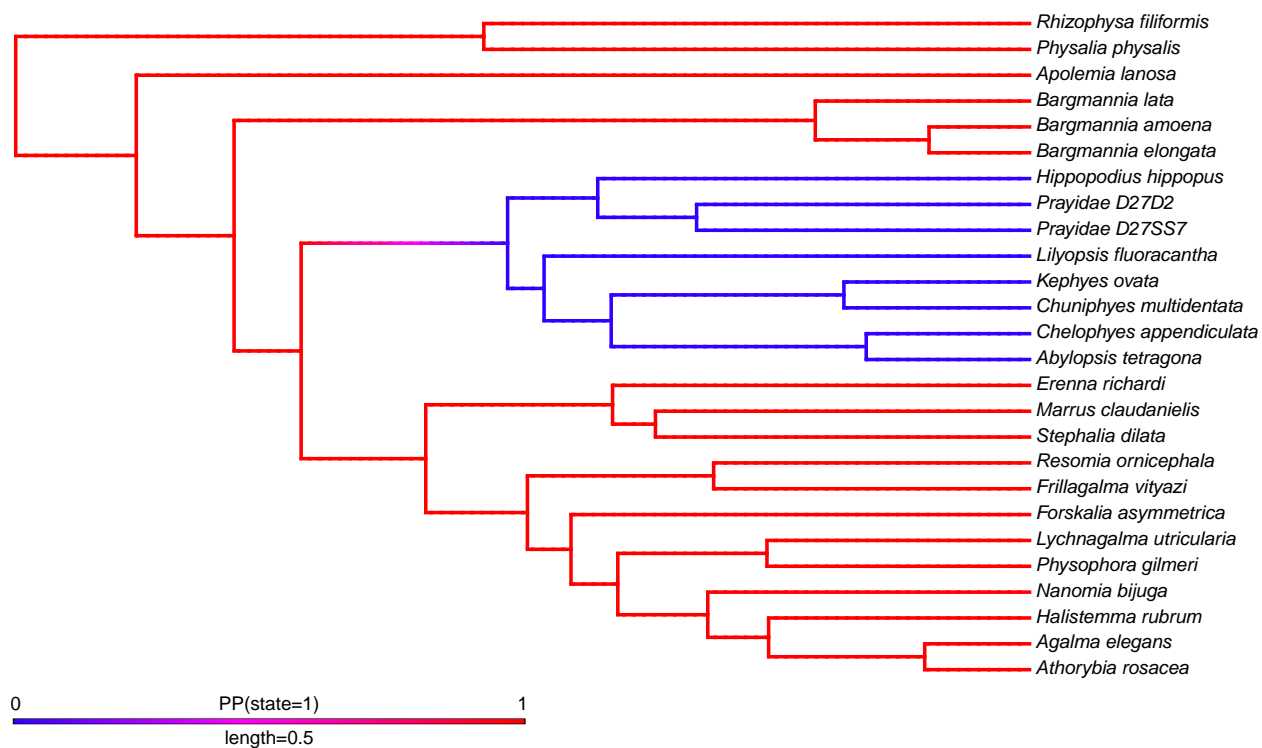
SIMMAP Position of Nectosome:



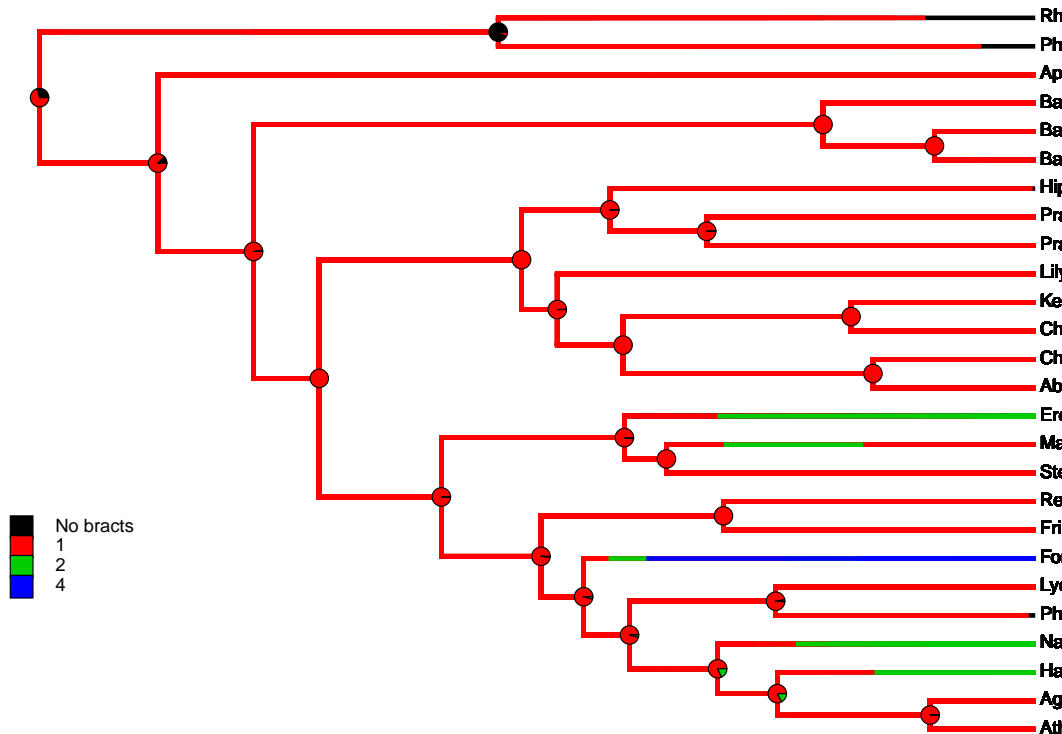
SIMMAP Nectophore number and types:



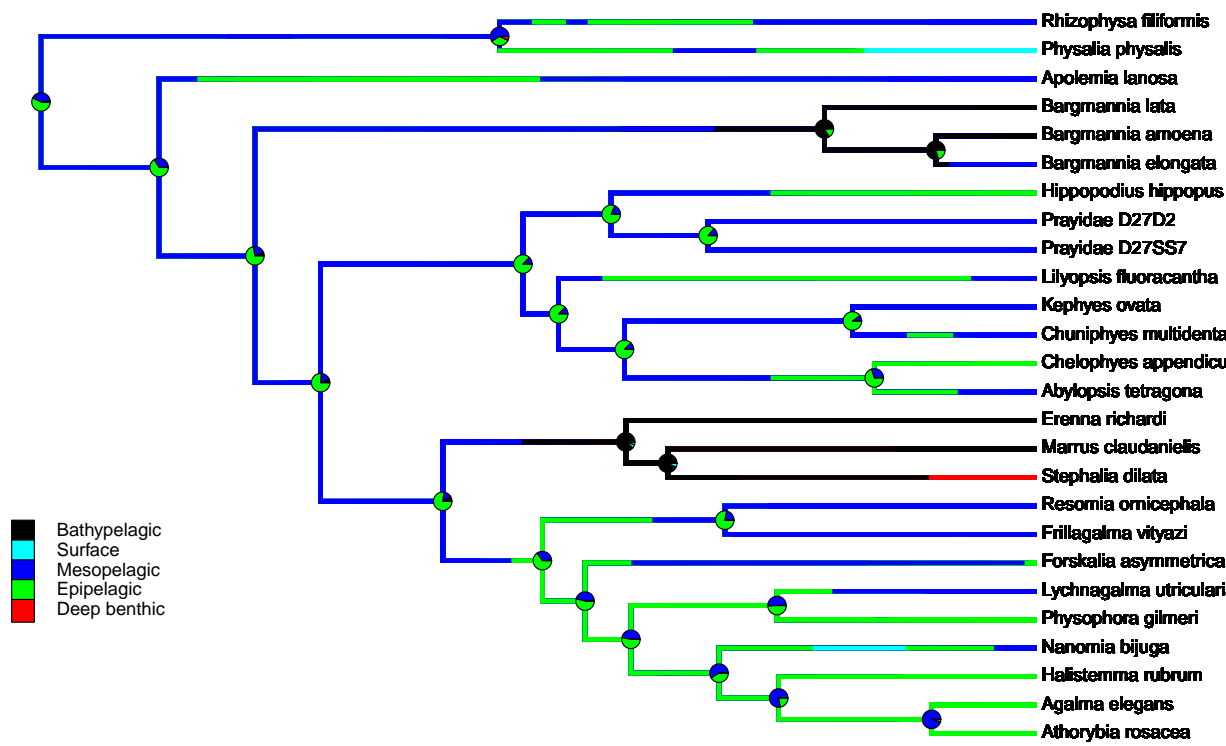
SIMMAP Presence of Pneumatophore:



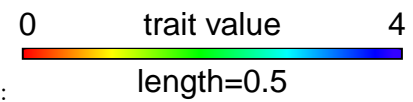
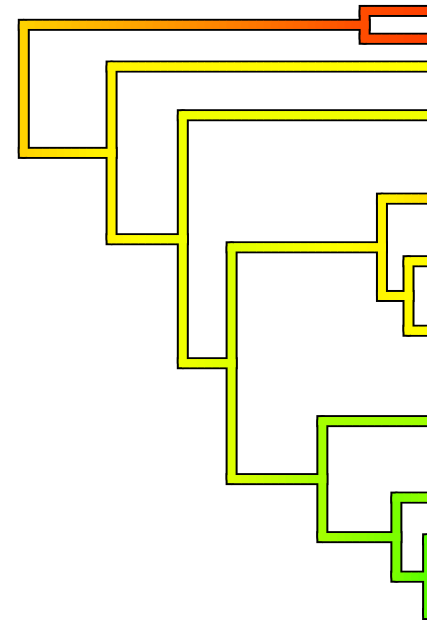
It is not clear whether or not the stem group of siphonophores had a pneumatophore.



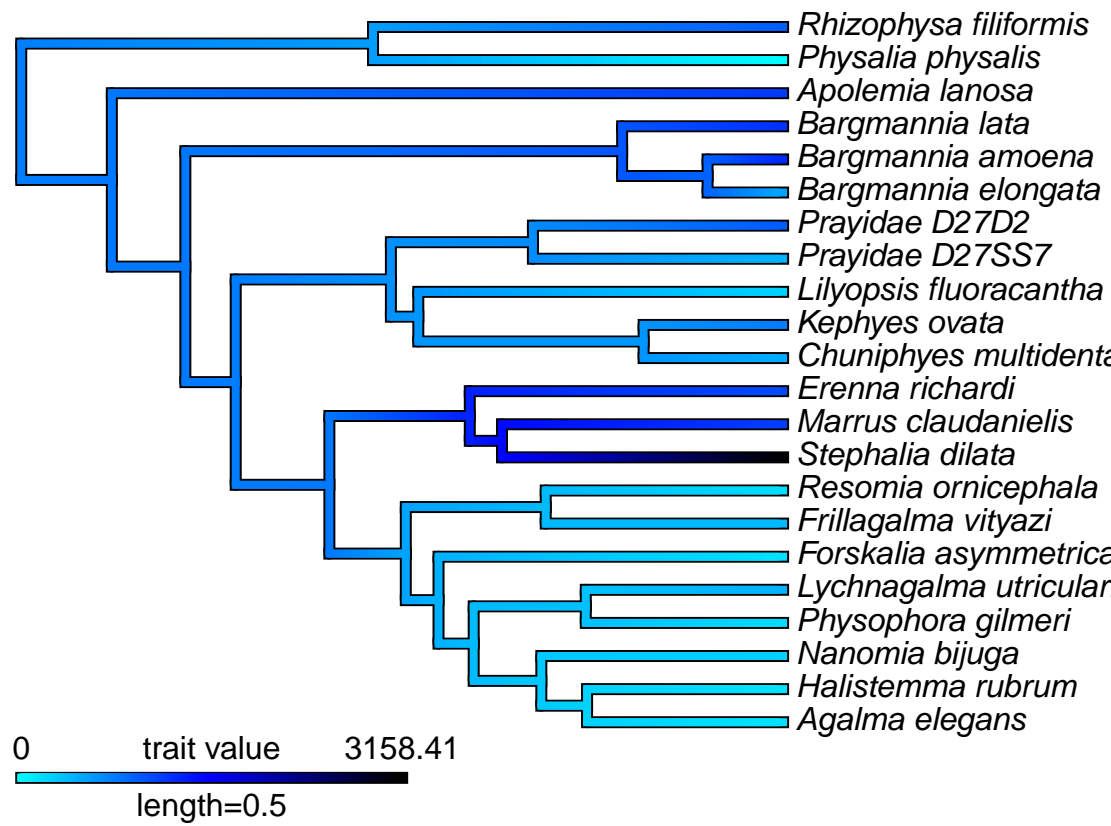
SIMMAP Number of Bract types:



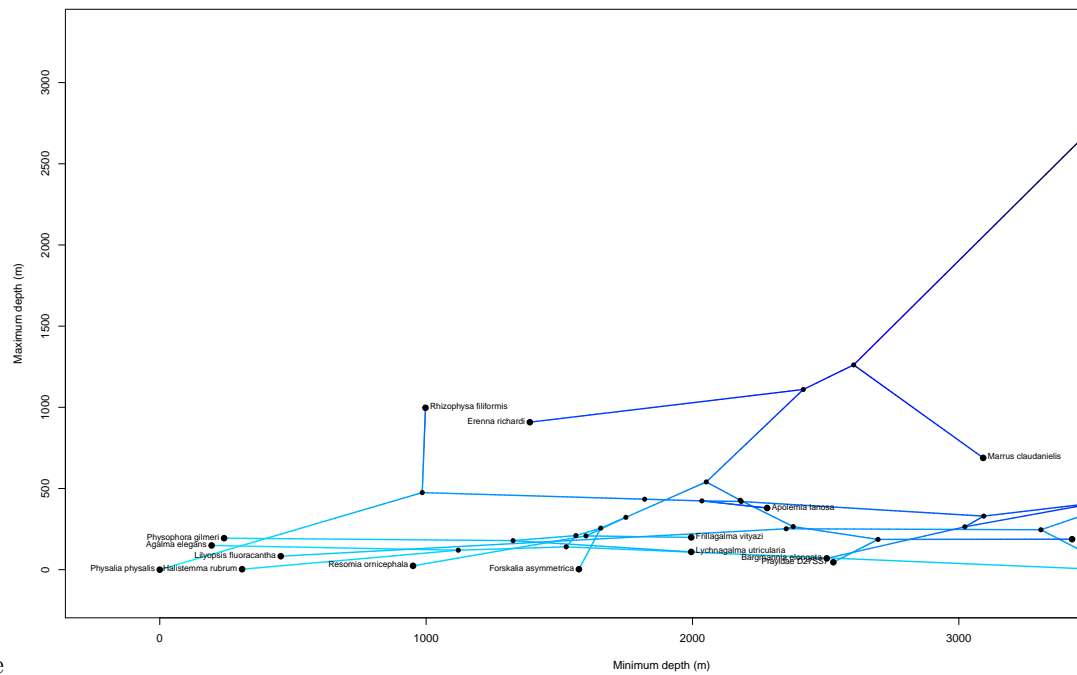
SIMMAP Habitat:



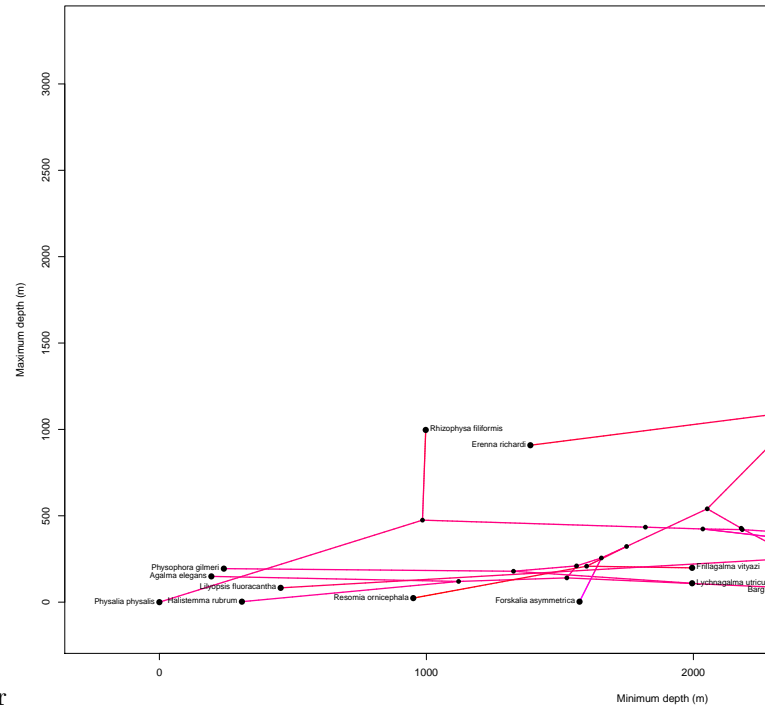
Continuous traits: Brownian motion reconstructions Number of bract types reconstruction:
Trait = Number of Bract Types



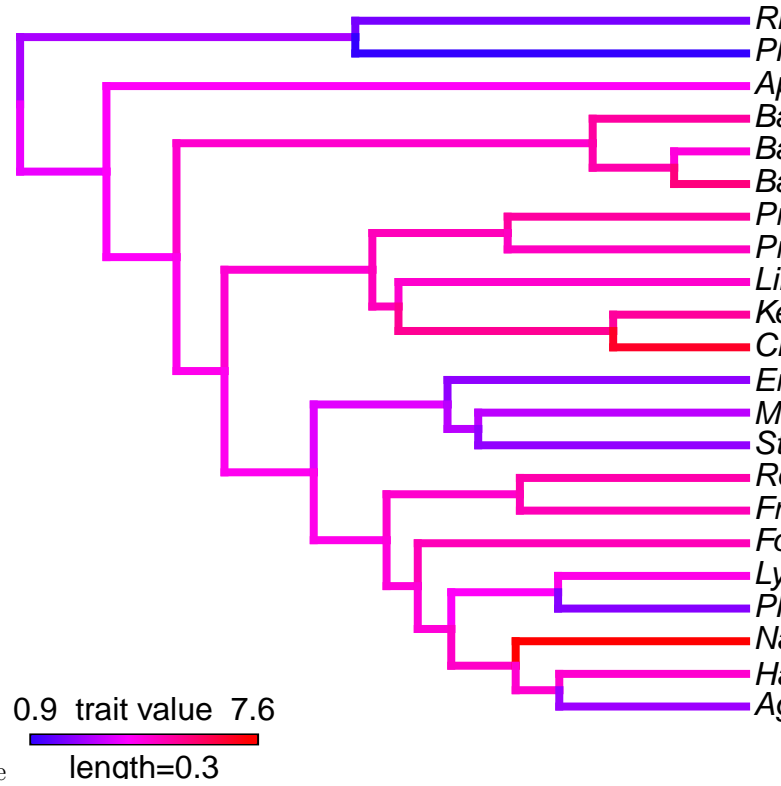
Median depth reconstruction:



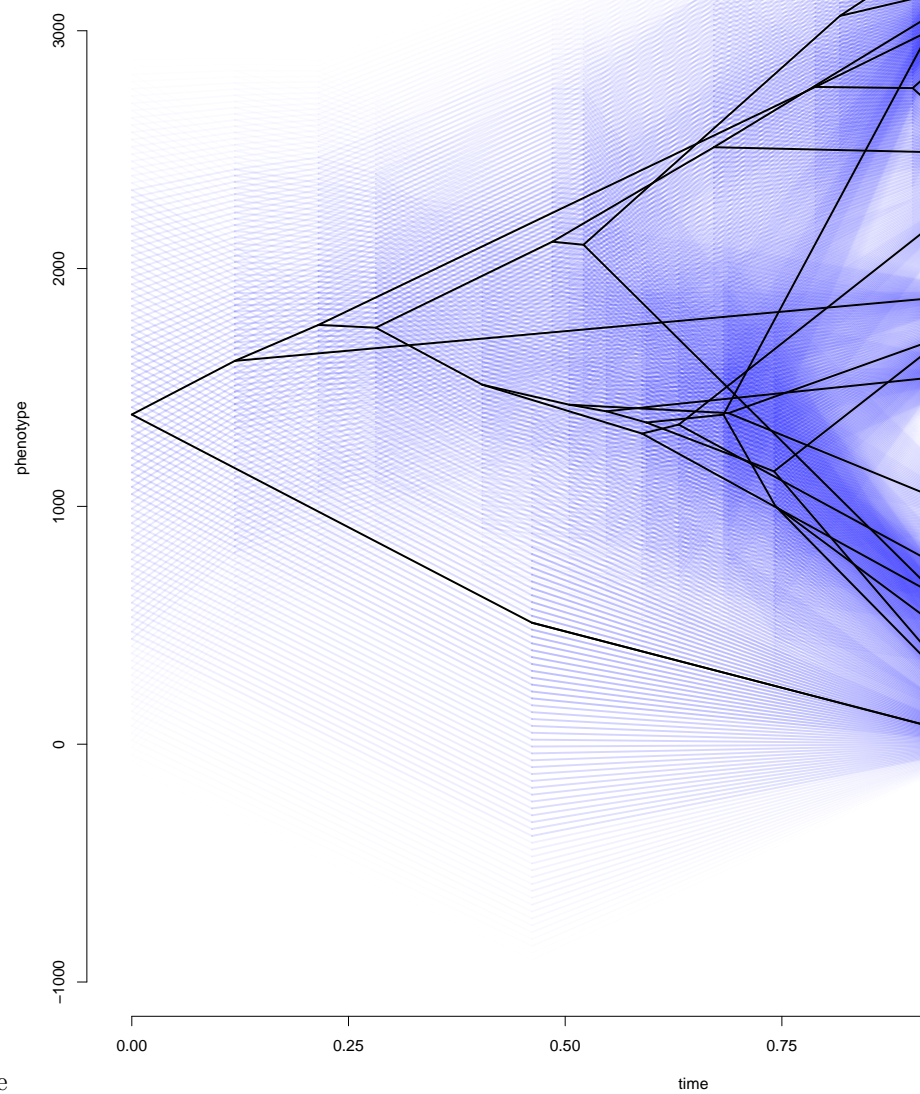
Bathymetrics phylomorphospace



Bathymetrics phylomorphospace with time from root as color



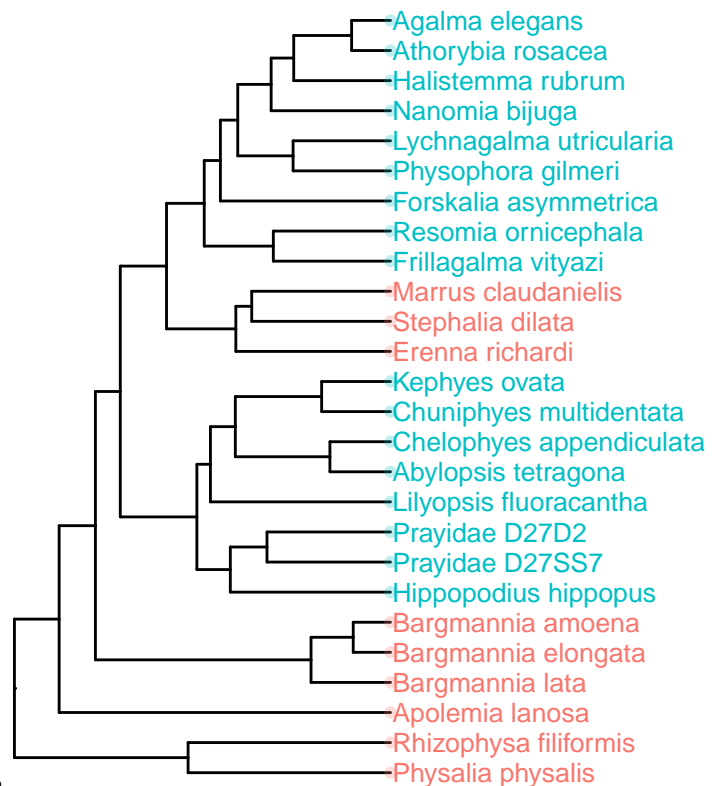
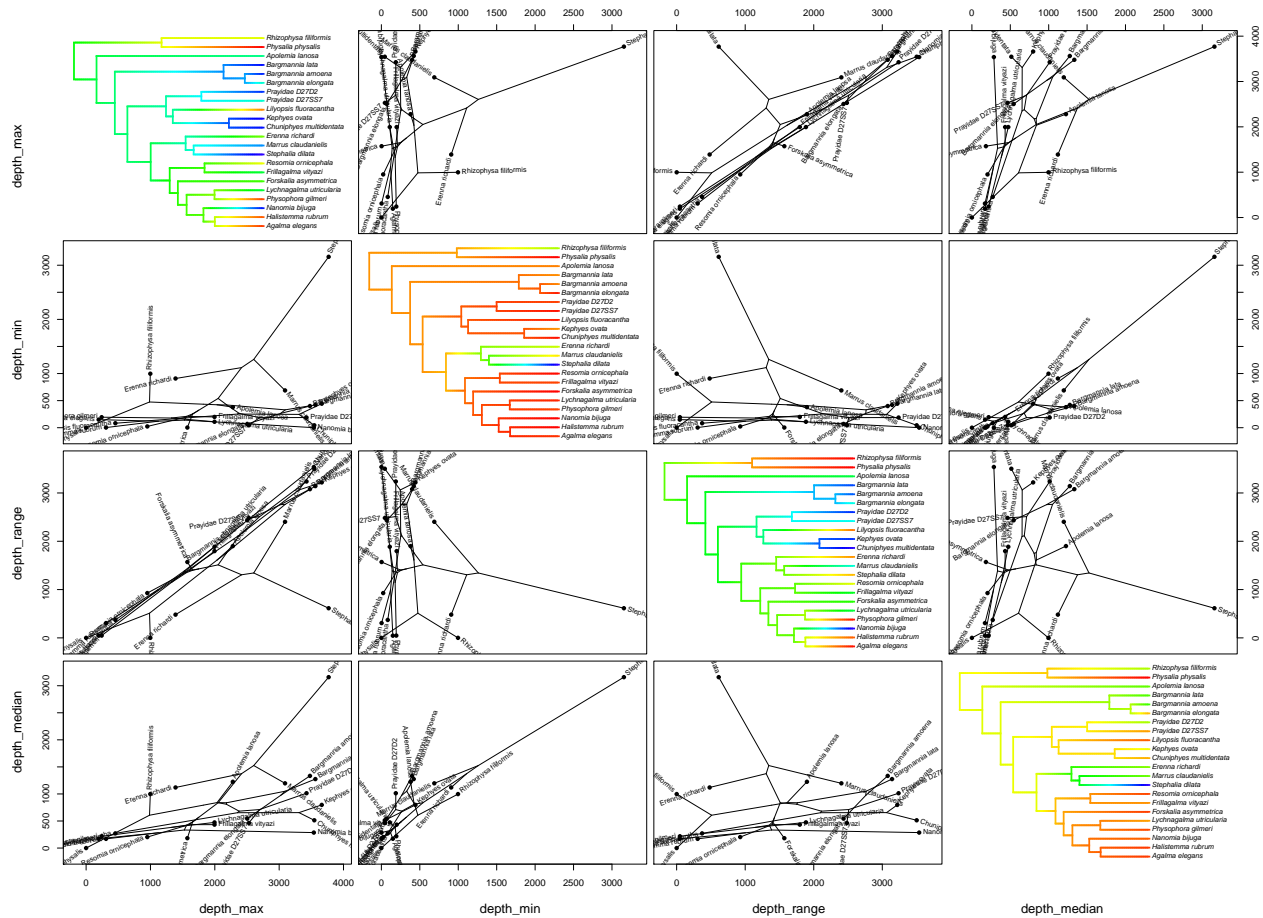
Abundance of each taxon in the Monterey Bay sampling site



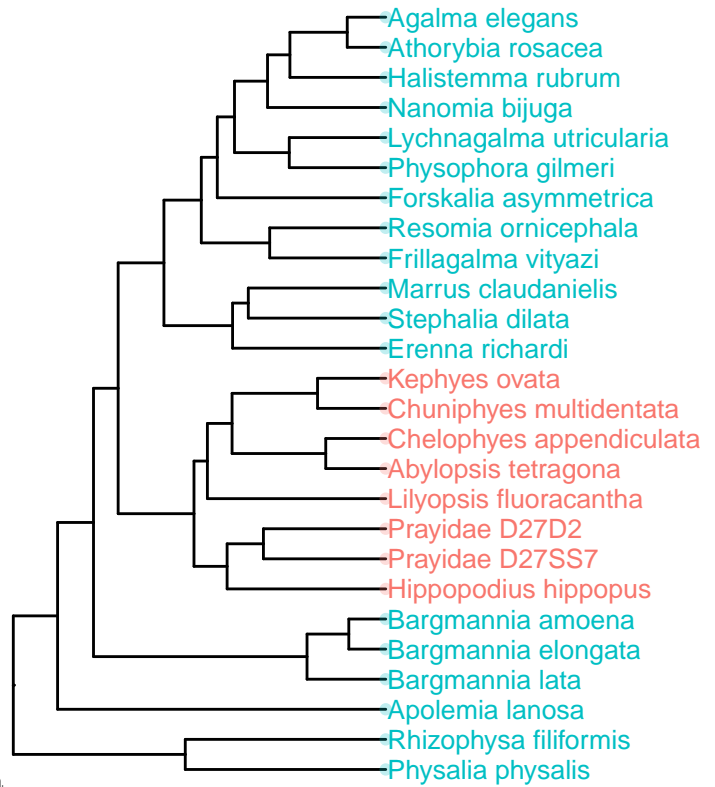
Uncertainty inclusive traitgram for depth range

Bathymetrics scattergram array

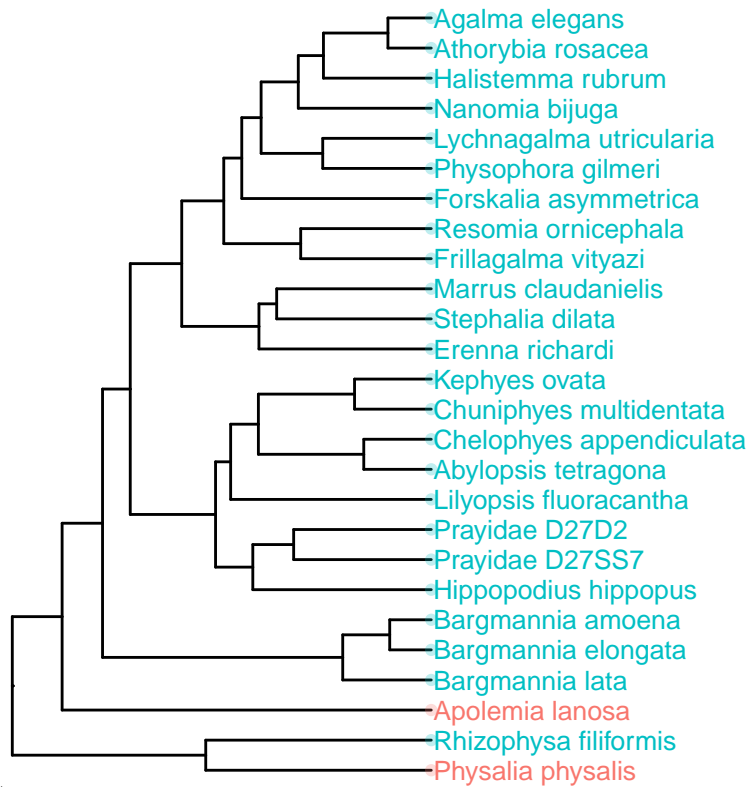
Computing multidimensional phylogenetic scatterplot matrix...



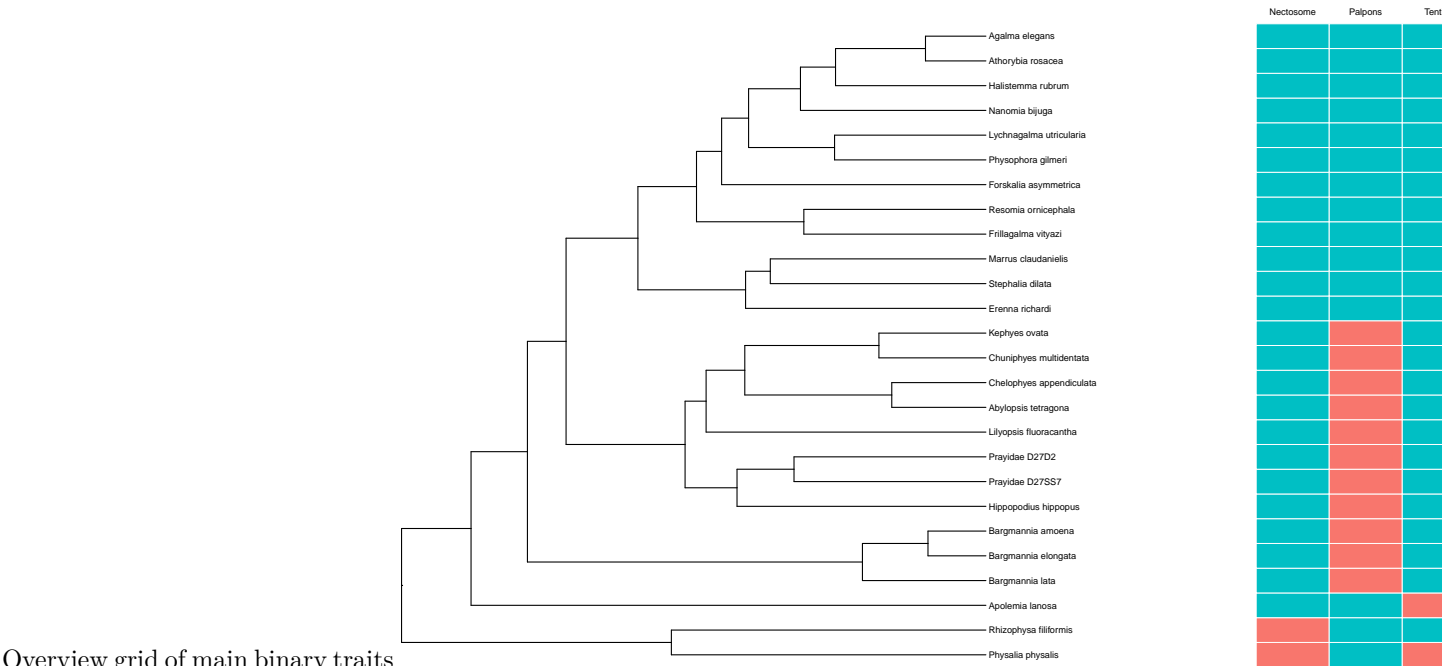
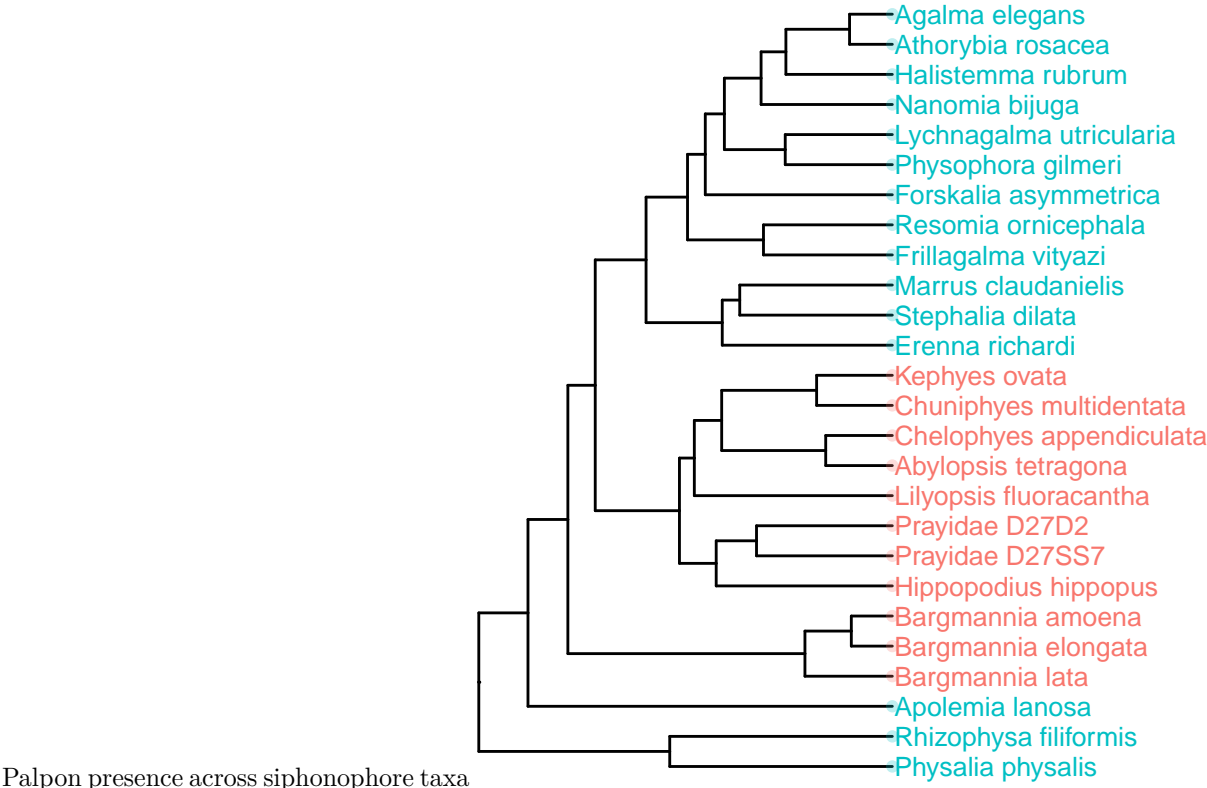
Distribution of sex across siphonophore taxa



Pneumatophore presence across siphonophore taxa



Tentilla presence across siphonophore taxa



Phylogenetic signal in the character data Agnostic branch length tree generation:

Phylogenetic signal in bract number

```
##          K PIC.variance.obs PIC.variance.rnd.mean PIC.variance.P
## 1 0.8009669      1.157887      1.949337      0.049
## PIC.variance.Z
## 1      -1.222729
```

```
##
## Call:
## physignal(A = bracts, phy = ultratree)
##
##
## Observed Phylogenetic Signal (K): 0.801
##
## P-value: 0.06
##
## Based on 1000 random permutations
```

Phylogenetic signal in Binary Traits

	K	PIC.variance.obs	PIC.variance.rnd.mean
Nectosome	4.078447	0.03981266	0.2244019
Palpons	3.146148	0.10883086	0.7799207
Tentilla	2.108915	0.07847782	0.2228660
Pneumatophore	3.367488	0.09051674	0.6826861

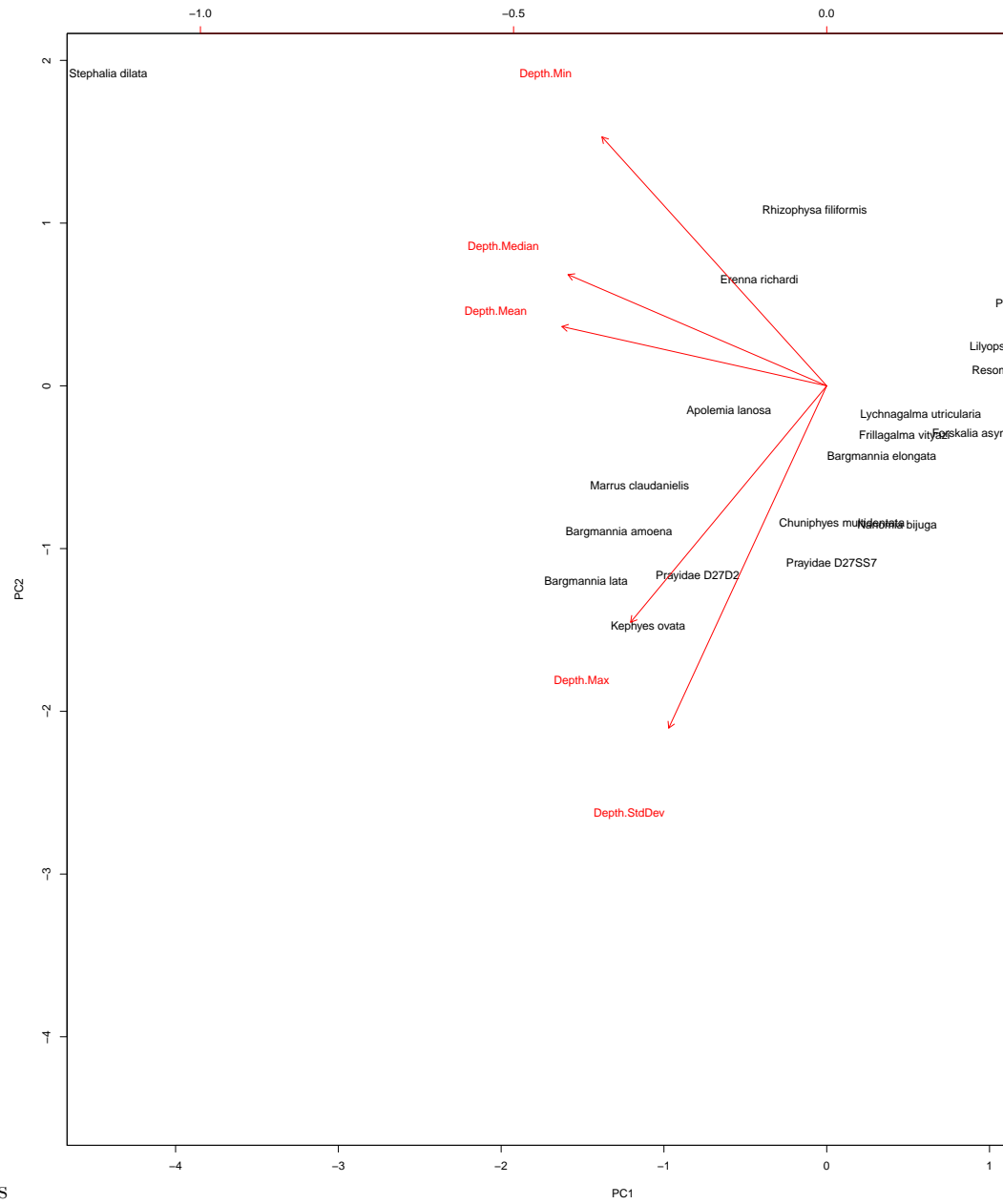
	PIC.variance.P	PIC.variance.Z
Nectosome	0.001	-2.348729
Palpons	0.001	-4.426048
Tentilla	0.008	-1.780424
Pneumatophore	0.001	-3.971181

Phylogenetic signal in VARS bathymetrics

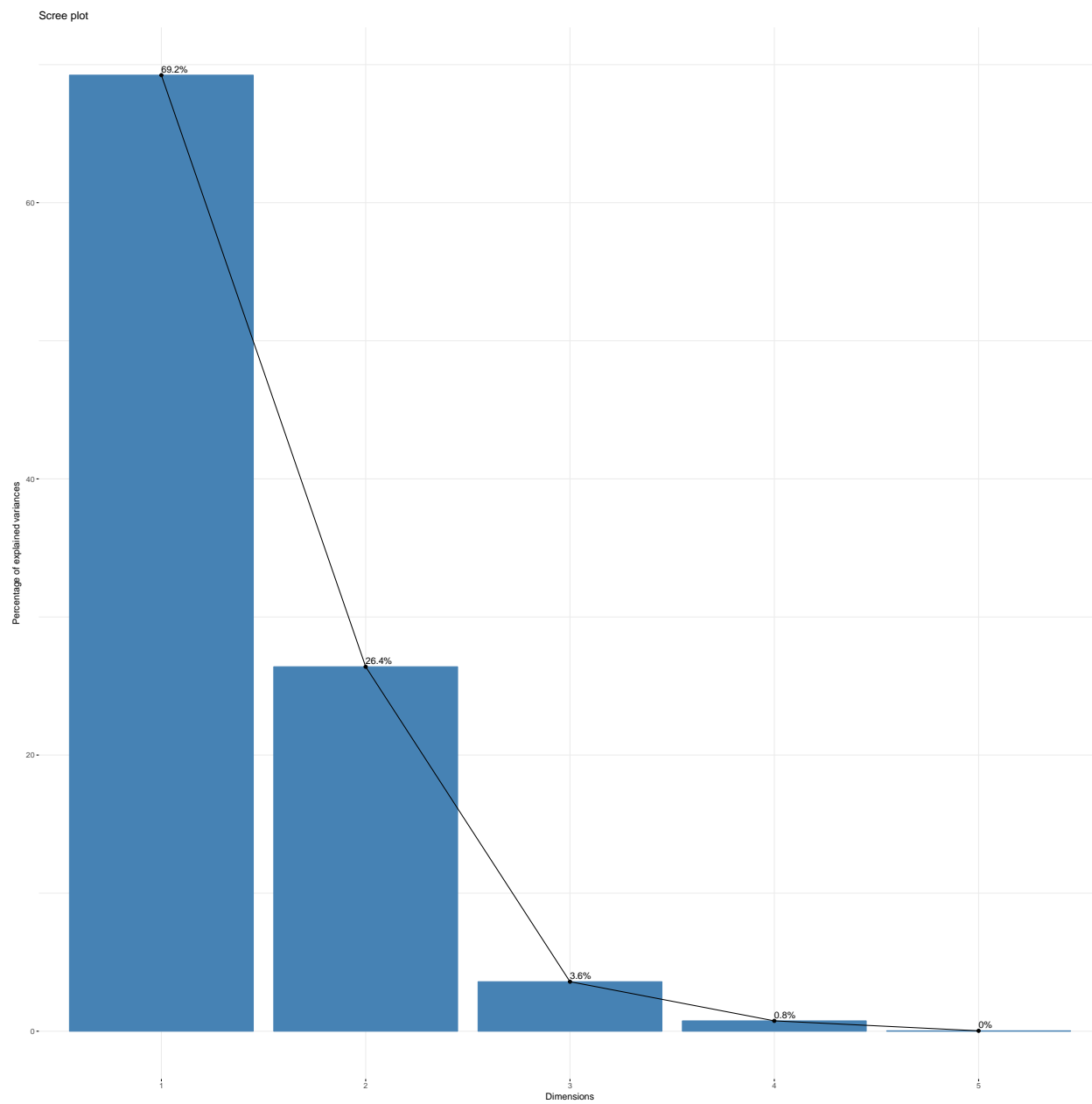
```
##
## Call:
## physignal(A = dpruned_data[, c(14, 15, 16, 18, 19)], phy = dpruned_tree)
##
##
## Observed Phylogenetic Signal (K): 0.713
##
## P-value: 0.041
##
## Based on 1000 random permutations
```

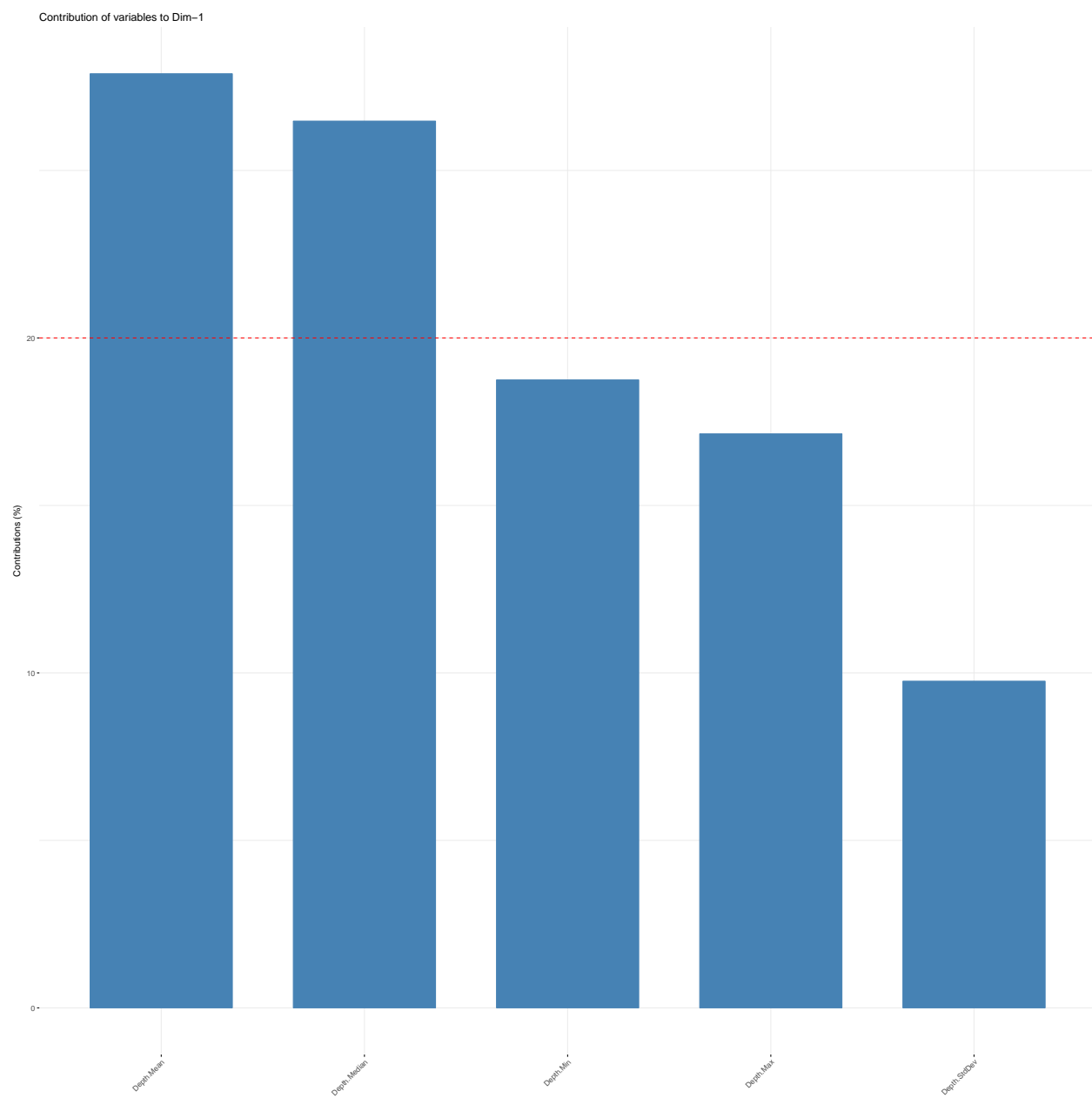
	K	PIC.variance.obs	PIC.variance.rnd.mean
Depth.Median	0.7102056	874545.3	1310039.0
Depth.Mean	0.6810206	1019335.8	1463498.8
Depth.StdDev	0.5889906	137873.8	168936.5
Depth.Max	0.7249934	3266103.9	4877727.2
Depth.Min	0.7287560	828880.7	1290988.0

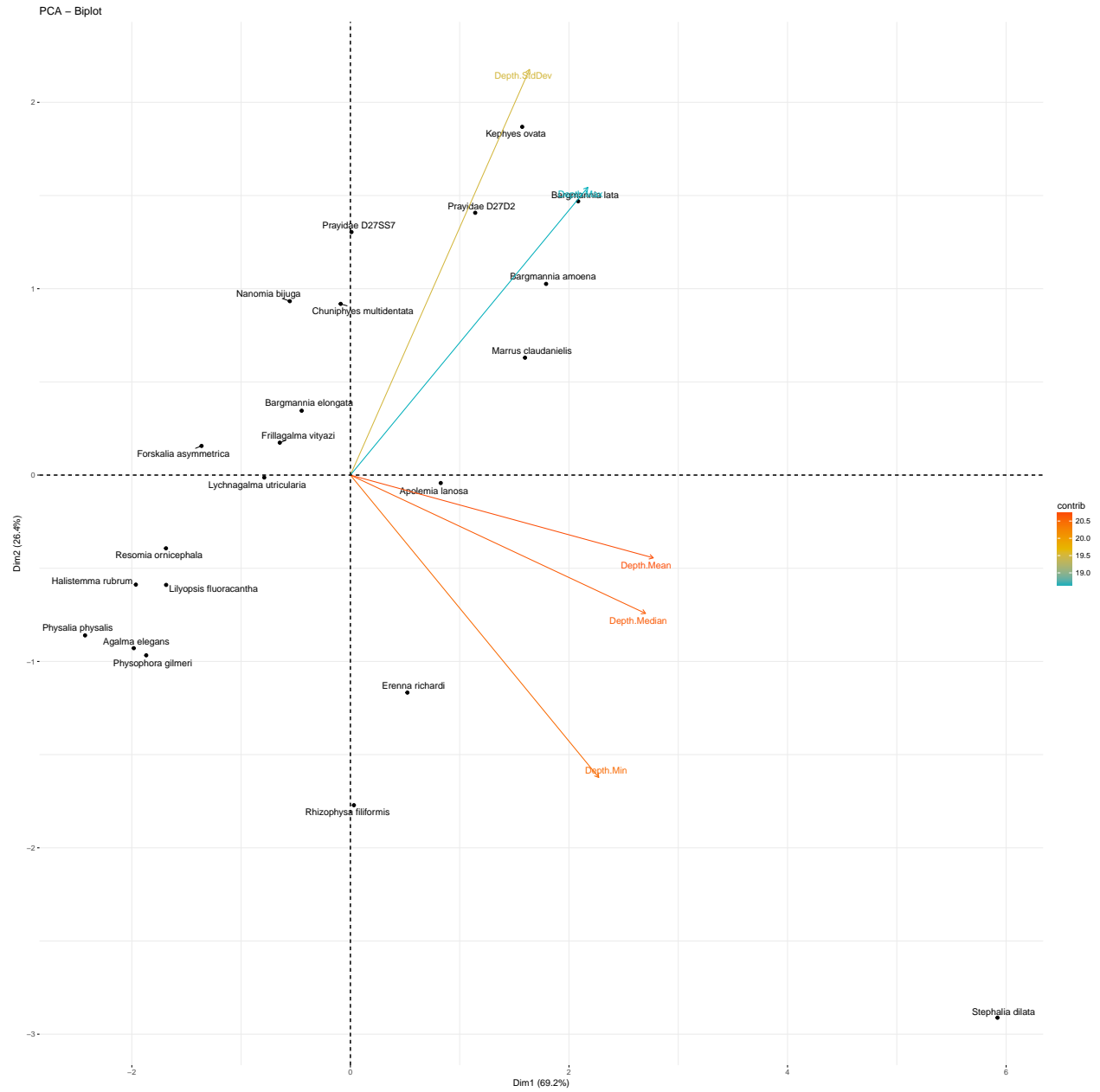
	PIC.variance.P	PIC.variance.Z
Depth.Median	0.082	-1.0008803
Depth.Mean	0.100	-1.0180552
Depth.StdDev	0.215	-0.7708171
Depth.Max	0.054	-1.5530691
Depth.Min	0.120	-0.9146162

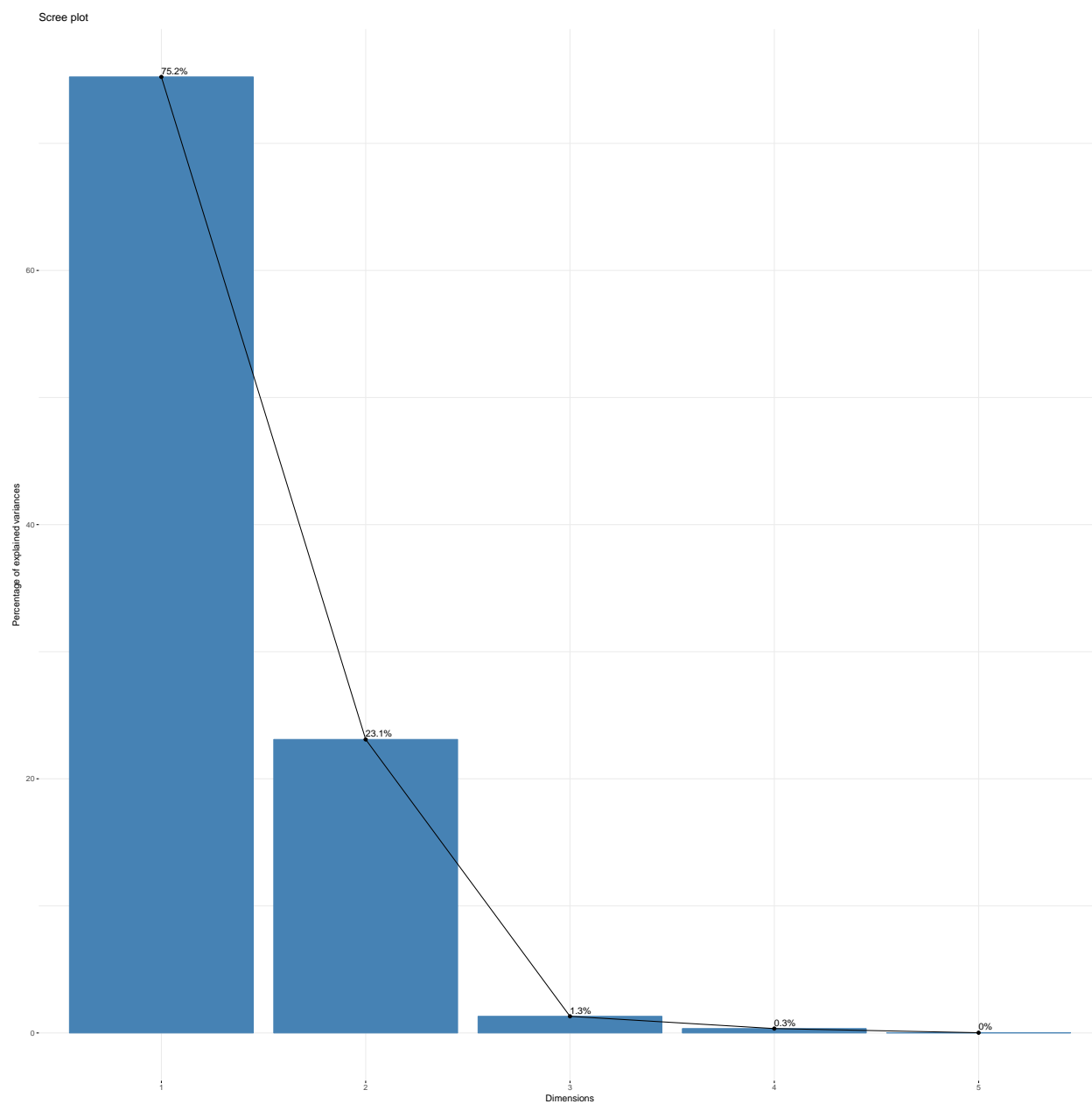


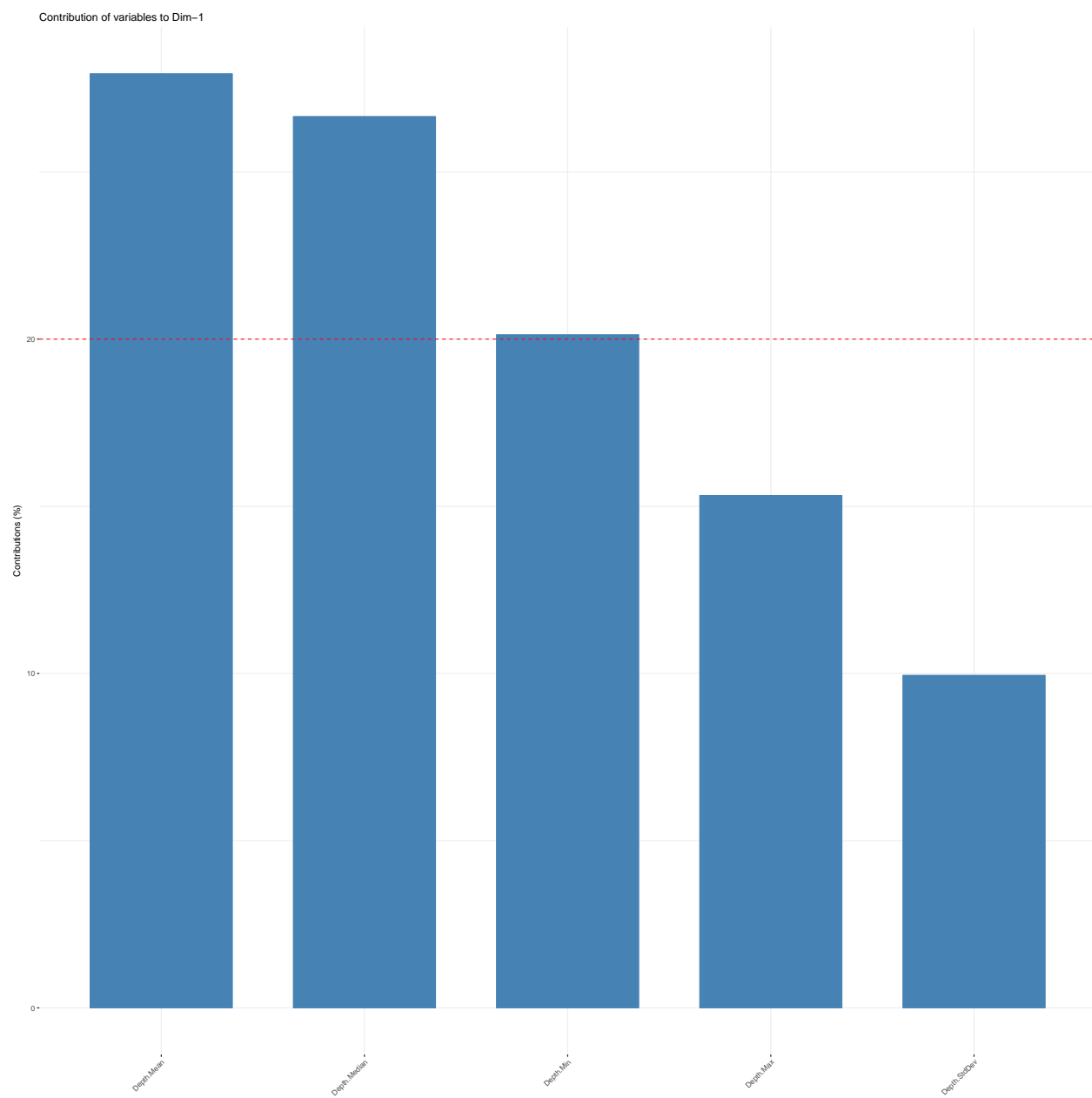
Phylogenetic PCA for bathymetrics

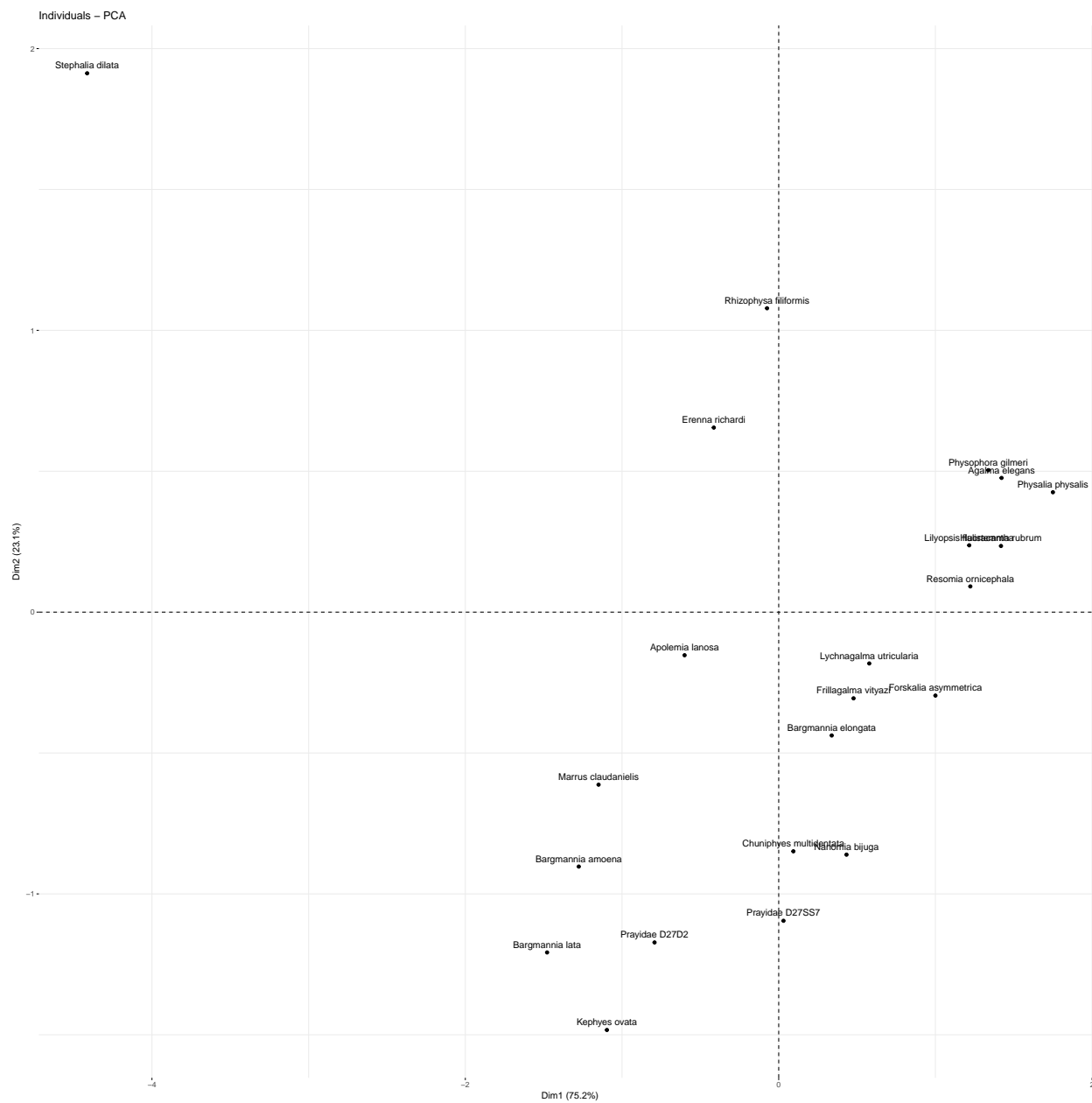












Phylogenetic ANOVA for depth

Each phylogenetic ANOVA compares variance of depth (continuous variable) within and between groups clustered by their categorical biological traits.

```
## [1] "Depth vs Sex Distribution"
```

```
## $F
```

```
## [1] 10.48139
```

```
##
```

```
## $Pf
```

```
## [1] 0.056
```

```
##
```

```
## $T
```

```
##          Dioecious Monoecious
```

```
## Dioecious 0.000000 3.237497
```

```

## Monoecious -3.237497  0.000000
##
## $method
## [1] "holm"
##
## $Pt
##           Dioecious Monoecious
## Dioecious      1.000      0.056
## Monoecious      0.056      1.000
## [1] "Depth vs Nectosome"
## $F
## [1] 0.2358588
##
## $Pf
## [1] 0.796
##
## $T
##           0          1
## 0 0.000000 -0.485653
## 1 0.485653  0.000000
##
## $method
## [1] "holm"
##
## $Pt
##           0          1
## 0 1.000 0.796
## 1 0.796 1.000
## [1] "Depth vs Nectophore Types and Number"
## $F
## [1] 0.156464
##
## $Pf
## [1] 0.98
##
## $T
##           Multiple of one type None One of one type
## Multiple of one type           NA  NA              NA
## None                        NA  NA              NA
## One of one type             NA  NA              NA
## Two of one type             NA  NA              NA
## Two of two types            NA  NA              NA
##           Two of one type Two of two types
## Multiple of one type      NA              NA
## None                      NA              NA
## One of one type           NA              NA
## Two of one type           NA              NA
## Two of two types          NA              NA
##
## $method
## [1] "holm"
##

```

```

## $Pt
##           Multiple of one type None One of one type
## Multiple of one type           NA  NA              NA
## None                          NA  NA              NA
## One of one type               NA  NA              NA
## Two of one type               NA  NA              NA
## Two of two types              NA  NA              NA
##           Two of one type Two of two types
## Multiple of one type           NA              NA
## None                          NA              NA
## One of one type               NA              NA
## Two of one type               NA              NA
## Two of two types              NA              NA

## [1] "Depth vs Nectosome Position"

## $F
## [1] 1.238642
##
## $Pf
## [1] 0.594
##
## $T
##           Dorsal      None      Ventral
## Dorsal  0.0000000 -0.4636838 -1.4922990
## None    0.4636838  0.0000000 -0.6838791
## Ventral 1.4922990  0.6838791  0.0000000
##
## $method
## [1] "holm"
##
## $Pt
##           Dorsal None Ventral
## Dorsal   1.000    1  0.831
## None     1.000    1  1.000
## Ventral  0.831    1  1.000

## [1] "Depth vs Palpons"

## $F
## [1] 0.05567054
##
## $Pf
## [1] 0.889
##
## $T
##           0      1
## 0  0.0000000 0.2359461
## 1 -0.2359461 0.0000000
##
## $method
## [1] "holm"
##
## $Pt
##           0      1
## 0  1.000 0.889

```



```

## 1 0.889 1.000
## [1] "Depth vs Tentilla"
## $F
## [1] 0.06009463
##
## $Pf
## [1] 0.873
##
## $T
##           0           1
## 0 0.0000000 -0.2451421
## 1 0.2451421  0.0000000
##
## $method
## [1] "holm"
##
## $Pt
##           0           1
## 0 1.000 0.873
## 1 0.873 1.000
## [1] "Depth vs Pneumatophore"
## $F
## [1] 0.1796993
##
## $Pf
## [1] 0.793
##
## $T
##           0           1
## 0 0.0000000 -0.4239096
## 1 0.4239096  0.0000000
##
## $method
## [1] "holm"
##
## $Pt
##           0           1
## 0 1.000 0.793
## 1 0.793 1.000
PGLS - Sex distribution
## -----
## | **Warning:                                     |
## |   User reports suggest that this method may frequently   |
## |   fail to find the ML solution. Please use with caution.   |
## |-----|
##
## Call:
## phylolm(formula = depth_median ~ dp_sex, data = as.data.frame(cbind(depth_median,
##   dp_sex)), phy = dpruned_tree, model = "BM", measurement_error = TRUE,
##   boot = 100)
##

```

```
##      AIC logLik
##    347.8 -169.9
##
## Parameter estimate(s) using ML:
## sigma2: 0.04476443
## sigma2_error: 299475.5
##
## Coefficients:
## (Intercept)      dp_sex
##    399.7538    805.7584

## Generalized least squares fit by REML
##   Model: dp_sex ~ depth_median
##   Data: NULL
##   Log-restricted-likelihood: -20.52555
##
## Coefficients:
## (Intercept) depth_median
## 0.0978229509 0.0004267556
##
## Degrees of freedom: 22 total; 20 residual
## Residual standard error: 0.4176998
```

Software versions

This manuscript was computed on Mon Oct 30 09:56:01 2017 with the following R package versions.

```
R version 3.4.1 (2017-06-30)
Platform: x86_64-apple-darwin15.6.0 (64-bit)
Running under: macOS Sierra 10.12.2
```

```
Matrix products: default
BLAS: /Library/Frameworks/R.framework/Versions/3.4/Resources/lib/libRblas.0.dylib
LAPACK: /Library/Frameworks/R.framework/Versions/3.4/Resources/lib/libRlapack.dylib
```

```
locale:
[1] en_GB.UTF-8/en_GB.UTF-8/en_GB.UTF-8/C/en_GB.UTF-8/en_GB.UTF-8
```

```
attached base packages:
[1] grid      parallel stats      graphics grDevices utils      datasets
[8] methods   base
```

```
other attached packages:
[1] bindrcpp_0.2      phylolm_2.5      geomorph_3.0.5    rgl_0.98.1
[5] adephylo_1.1-10   ade4_1.7-8       phylobase_0.8.4   geiger_2.0.6
[9] phangorn_2.2.0    phytools_0.6-20  picante_1.6-2     nlme_3.1-131
[13] vegan_2.4-4       lattice_0.20-35  permute_0.9-4     ape_4.1
[17] hutan_0.5.0       FactoMineR_1.38  factoextra_1.0.5  gridExtra_2.3
[21] seriation_1.2-2   fields_9.0       maps_3.2.0        spam_2.1-1
[25] dotCall64_0.9-04  ggtree_1.8.2     treeio_1.0.2      cowplot_0.8.0
[29] xtable_1.8-2      jsonlite_1.5     knitr_1.17        digest_0.6.12
[33] magrittr_1.5      forcats_0.2.0    stringr_1.2.0     dplyr_0.7.4
[37] purrr_0.2.3       readr_1.1.1      tidyr_0.7.1       tibble_1.3.4
[41] ggplot2_2.2.1     tidyverse_1.1.1
```

loaded via a namespace (and not attached):

[1] readxl_1.0.0	uuid_0.1-2
[3] backports_1.1.1	fastmatch_1.1-0
[5] plyr_1.8.4	igraph_1.1.2
[7] lazyeval_0.2.0	sp_1.2-5
[9] splines_3.4.1	rncl_0.8.2
[11] foreach_1.4.3	htmltools_0.3.6
[13] viridis_0.4.0	gdata_2.18.0
[15] cluster_2.0.6	gclus_1.3.1
[17] modelr_0.1.1	gmodels_2.16.2
[19] prettyunits_1.0.2	jpeg_0.1-8
[21] colorspace_1.3-2	rvest_0.3.2
[23] ggrepel_0.7.0	haven_1.1.0
[25] bindr_0.1	survival_2.41-3
[27] iterators_1.0.8	glue_1.1.1
[29] registry_0.3	gtable_0.2.0
[31] seqinr_3.4-5	kernlab_0.9-25
[33] prabclus_2.2-6	DEoptimR_1.0-8
[35] scales_0.5.0	mvtnorm_1.0-6
[37] DBI_0.7	Rcpp_0.12.13
[39] plotrix_3.6-6	viridisLite_0.2.0
[41] progress_1.1.2	spdep_0.6-15
[43] flashClust_1.01-2	foreign_0.8-69
[45] subplex_1.4-1	bold_0.5.0
[47] mclust_5.3	deSolve_1.20
[49] stats4_3.4.1	animation_2.5
[51] htmlwidgets_0.9	httr_1.3.1
[53] gplots_3.0.1	fpc_2.1-10
[55] modeltools_0.2-21	pkgconfig_2.0.1
[57] reshape_0.8.7	XML_3.98-1.9
[59] flexmix_2.3-14	deldir_0.1-14
[61] nnet_7.3-12	crul_0.4.0
[63] tidyselect_0.2.0	labeling_0.3
[65] rlang_0.1.2	reshape2_1.4.2
[67] munSELL_0.4.3	cellranger_1.1.0
[69] tools_3.4.1	broom_0.4.2
[71] evaluate_0.10.1	yaml_2.1.14
[73] robustbase_0.92-7	caTools_1.17.1
[75] dendextend_1.5.2	mime_0.5
[77] whisker_0.3-2	taxize_0.9.0
[79] adegenet_2.1.0	leaps_3.0
[81] xml2_1.1.1	compiler_3.4.1
[83] curl_2.8.1	clusterGeneration_1.3.4
[85] RNeXML_2.0.7	stringi_1.1.5
[87] highr_0.6	trimcluster_0.1-2
[89] Matrix_1.2-11	psych_1.7.8
[91] msm_1.6.4	LearnBayes_2.15
[93] combinat_0.0-8	data.table_1.10.4
[95] bitops_1.0-6	httpuv_1.3.5
[97] R6_2.2.2	TSP_1.1-5
[99] KernSmooth_2.23-15	codetools_0.2-15
[101] boot_1.3-20	MASS_7.3-47
[103] gtools_3.5.0	assertthat_0.2.0

[105]	rprojroot_1.2	mnormt_1.5-5
[107]	diptest_0.75-7	mgcv_1.8-22
[109]	expm_0.999-2	hms_0.3
[111]	quadprog_1.5-5	coda_0.19-1
[113]	class_7.3-14	rmarkdown_1.6
[115]	rvcheck_0.0.9	ggpubr_0.1.5
[117]	shiny_1.0.5	numDeriv_2016.8-1
[119]	scatterplot3d_0.3-40	lubridate_1.6.0

References

- Dunn C., Pugh P., Haddock S. 2005. Molecular Phylogenetics of the Siphonophora (Cnidaria), with Implications for the Evolution of Functional Specialization. *Systematic biology*. 54:916–935.
- Dunn C.W., Howison M., Zapata F. 2013. Agalma: an automated phylogenomics workflow. *BMC Bioinformatics*. 14:330.
- Lartillot N., Lepage T., Blanquart S. 2009. PhyloBayes 3: A bayesian software package for phylogenetic reconstruction and molecular dating. *Bioinformatics*. 25:2286–2288.
- Lartillot N., Philippe H. 2004. A bayesian mixture model for across-site heterogeneities in the amino-acid replacement process. *Molecular Biology and Evolution*. 21:1095–1109.
- Yu G., Smith D.K., Zhu H., Guan Y., Lam T.T.-Y. 2016. ggtree: an r package for visualization and annotation of phylogenetic trees with their covariates and other associated data. *Methods in Ecology and Evolution*.